ACS OMEGA

Open Access

http://pubs.acs.org/journal/acsodf

Article

Co-Delivery of Naringin and Ciprofloxacin by Oleic Acid Lipid Core Encapsulated in Carboxymethyl Chitosan/Alginate Nanoparticle Composite for Enhanced Antimicrobial Activity

Tahani M. Almeleebia, Md Habban Akhter,* Habibullah Khalilullah,* Mohammad Akhlaquer Rahman, Sarfaraz Ahmad, Nawazish Alam, Md Sajid Ali, Gyas Khan, Ibrahim Mufadhi M. Alanazi, Naiyer Shahzad, and Amnah Alalmaie

Cite This: *ACS Omega* 2024, 9, 6845−6860

Read Online

ACCESS | Metrics & More | Article Recommendations

ABSTRACT: A novel combination of antibiotic, ciprofloxacin (CIP) with herbal counterpart naringin (NAR) was encapsulated by an oleic acid lipid core and carboxymethyl chitosan (CM−CS)/Alginate (AG) nanoparticle composite (CIP + NAR−CM−CS/AG−NPs) for improved antimicrobial efficacy of antibiotic. Herein, this study explored the design and preparation of a composite system that enables to deliver both CIP and NAR from the oleic acid lipid core of CM−CS/AG nanoparticles using a nonsolvent ionic gelation technique. The nanoparticles (NPs) were fabricated with improved long-acting antimicrobial activity against *E. coli* and *S. aureus*. The optimized composition was investigated for physicochemical properties particle size, particle distribution, and ζ−potential. A diverse array of analytical tools was employed to characterize the optimized formulation including DSC, XRD, Malvern Zetasizer for particle size, ζ−potential, TEM, and SEM. Further, the preparation was investigated for % drug release, flux determination, antioxidant, and antimicrobial activity. The formulation stability was tested for 90 days and also evaluated formulation stability in fetal bovine serum to inspect the modification in physicochemical characteristics. NPs size was determined at 85 nm, PDI, and ζ−potential was recorded at 0.318, and 0.7 ± 0.4 mV. The % CIP and NAR entrapment efficiency and % loading were incurred as 91 ± 1.9, and 89.5 ± 1.2; 11.5 ± 0.6, and 10.8 ± 0.5%, respectively. The drug release erupted in the beginning phase followed by sustained and prolonged release for 48 h. The analytical experiments by DSC ensured the noninteracting and safe use of excipients in combination. X−ray studies demonstrated the amorphous state of the drug in the formulation. The insignificant alteration of formulation characteristics in FBS suggested stable and robust preparation. Storage stability of the developed formulation ensured consistent and uniform stability for three months. The DPPH assays demonstrated that NAR had good antioxidant capacity and supported improving antimicrobial activity of CIP. The hemolytic test suggested the developed formulation was compatible and caused insignificant RBC destruction. The in-house built formulation CIP + NAR−CM−CS/AG−NPs significantly improved the antimicrobial activity compared to CIP alone, offering a novel choice in antimicrobial application.

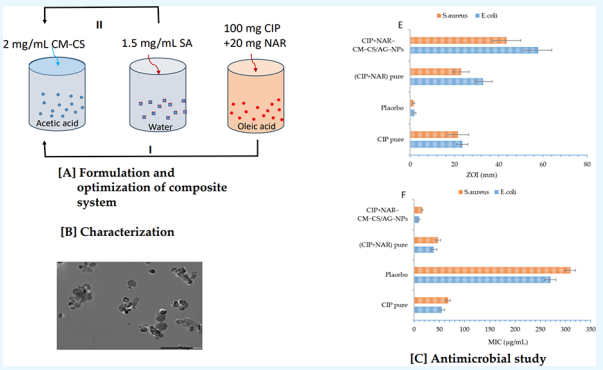

INTRODUCTION

The irrational, unjustified irregular, and continuous application of antibiotics may lead to the emergence of resistance toward multiple pathogenic microbes. The rate of developing new resistance among pathogens is high as compared to the discovery of new antibiotics jeopardizing a life.[1] Thus, there is an unmet need to develop new antimicrobial agents that enable suppression of the frequent use of antibiotics or reduction of the dose of antibiotics and combat resistance development. In view of this, scientists are ready to isolate, and identify bioactive products, and formulate either alone or in combination with antibiotics in a suitable nanocarrier to contend the antibiotic resistance.[2] Antibacterial resistance has been one of the most important obstacles in the treatment of bacterial disease for a few decades, bothering advances in healthcare professionals and industry. The growing rate of drug resistance toward antibiotics for human use is obligating innovators, and researchers to the

Received: October 18, 2023
Revised: January 4, 2024
Accepted: January 10, 2024
Published: February 2, 2024

https://doi.org/10.1021/acsomega.3c08200
ACS Omega 2024, 9, 6845−6860

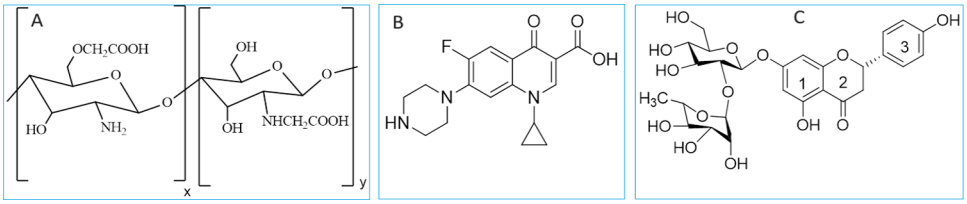

Figure 1. Chemical structure of carboxymethyl chitosan (A), ciprofloxacin (B), and naringin (C).

safe and effective use of phytomedicines as an alternate option in combination with antibiotics against microbial infection compelling researchers to promote the use of phytochemicals as an alternative.[3] Furthermore, the bacterial resistance has not been reported yet toward the use of phytochemicals.

Escherichia coli (E. coli) is a Gram-negative bacteria that can grow both in aerobic and anaerobic conditions in a variety of materials such as liquid or solid under a wide temperature range. It is an important family member of the intestinal microbiomes of humans and mammals. Apart from their application in DNA recombinant technology, they are highly versatile, virulent, and cause a diverse range of intestinal ailments. It colonizes new infants born within a short time. It is capable of causing infections in the gastrointestinal, urinary, and respiratory tract. The most common infections caused by them are diarrhea, dysentery, meningitis, and sepsis.[4] *Staphylococcus aureus (S. aureus)* is a highly resistant strain of bacteria causing endocarditis, sepsis, pneumonia, and toxic shock syndrome in humans and mammals. The α-toxin secreted by *S. aureus* may cause skin inflammation and necrotic pneumonia in animals.[6] The bacteria have well-established physiological machinery, signaling pathways, and virulence rate in causing infection.

The discovery and development of novel antimicrobial agents against broad-spectrum bacteria is a compelling need to overcome multidrug resistance. Several obstacles in the drug discovery path including long time and patience in research and uncertainty in getting positive outcomes in concern to safety and efficacy create hurdles for scientist.[7]

Opting for an alternate approach to enhance the existing drug efficacy is an unmet need of the day. This could be possible by implementing the recent advanced techniques based on nanotechnology greatly helpful in improving the biological activity and efficacy of the developed formulation.[8]

Kashef et al.[5] developed noisome vesicles loaded with ciprofloxacin for combating microbial and antibiofilm formation against *S. aureus*. They developed two noisome preparations of ciprofloxacin applying thin film hydration techniques and tested against multiple *S. aureus* isolates using disk diffusion techniques. First and second niosome formulations inhibited ciprofloxacin MIC by 2 times in 4-isolates, and by 8−32-fold. The minimum inhibitory concentrations (MIC) were estimated for ciprofloxacin-resistant and biofilm-forming isolates through the agar dilution method. Ciprofloxacin niosomes successfully suppressed biofilm formation by 58% and their eradication by 62% among the investigated isolates.

Polysaccharides having unique features of physicochemical and biological characteristics of biocompatibility, biodegradability, no toxicity, and drug carrier have been widely used in biomedical and engineering applications. Polysaccharide has a natural activity for several many diseases varying from bacterial, antitumor, antioxidant, and antidiabetic.[9,10]

Chitosan is an FDA-approved natural polysaccharide obtained from the deacetylation of chitin in alkaline conditions. It is a buildup of two basic units of D-glucosamine and N-acetyl glucosamine. The poor aqueous solubility, rapid adsorption, and swelling in aqueous media may cause faster drug liberation in water limiting the use of chitosan. Carboxymethyl cellulose is a substituted product of chitosan or chitin with carboxymethyl group ($-CH_2-COOH$) introduced at the amino or hydroxyl active terminal. This substitution enhances the solubility of chitosan at neutral pH. Carboxymethyl chitosan (CM−CS) has wide applications in biomedical and pharmaceutical sciences including emulsifiers, thickening agents, drug carriers, adsorption, permeation enhancer, and mucoadhesiveness (Figure 1A). It interacts actively with biological cells/tissues and promotes regeneration, and tissue growth. Besides these, CM−CS has antimicrobial, antifungal, anti-inflammatory, antitumor, tissue engineering, diagnostics, and advanced drug delivery technologies.[11−13] CM−CS prevents biofilm formation and adherence of bacterial strains of both Gram-positive and Gram-negative bacteria, resulting in reduced cell-to-cell interaction and microbial floccules formed. Further, the amino group in CM−CS gets protonated in the physiological media and has a high affinity to bind with anionic group microbes and inhibit.[14] Alginate is an anionic water-soluble linear polysaccharide having α-L-guluronic acid (G-block) and β-D-mannuronic acid (M-block) two monomer units obtained from brown algae. The divalent metal ion such as Ca^{2+} or Mg^{2+} has high affinity due to ionic interactions and is strongly bound with the G-block of alginate, resulting in the formation of a cross-linked 3D network that appears as an "egg box model". The alginate blocks' composition and their sequence may affect the physicochemical properties of the compound. The aqueous solubility of alginate helps make stable ionic gelation in proximity with multivalent ions Ca^{2+}, Mg^{2+}, or Zn^{2+}. Due to having gelling properties and biocompatibility, it is preferred in medicine, cosmetics, pharmaceuticals, bioengineering, and food products.[15,16] The profound driving concept of nanocomposite formation relies on the cationic or neutral carboxymethyl chitosan forming polyelectrolyte complex with alginate molecule via ionic liaison between amines and the carboxyl functional group of chitosan and alginate molecule. The dissolved drugs in oleic acid are sandwiched between two biopolymer layers. The polyelectrolyte complex shields entrapped drugs more expeditiously than either of the biopolymers alone.[17] Owing to biofriendly applications and lack of potential or hazardous toxic effects, the use of nutraceutical or herbal-based products is growing nowadays, which enables attention to develop more effective and safer products. A nanoparticle offers a novel technology-based platform for drug delivery to the individual cell level that helps expedite the recovery of a disease in a precise manner. The surface tuning and multifunctionality through manipulating the nanoparticle surface more specific and challenging ailments could be treated by developing smart nanodrug delivery systems bearing macromolecules, biological products, therapeutic agents, and/or various plant-based active moieties. Phytochem-

https://doi.org/10.1021/acsomega.3c08200
ACS Omega 2024, 9, 6845−6860

Table 1. Formulation (NC1−NC8) Characterization Parameters, Particle Size, PDI, Zeta Potential, % Drug Encapsulation, and % Loading

				% encapsulation		% loading	
formulas code	particle size (nm)	PDI	zeta potential (mV)	CIP	NAR	CIP	NAR
NC1	50 ± 2.6	0.507	+0.3 ± 0.1	42 ± 2.7	39 ± 0.8	8.3 ± 0.6	8.4 ± 0.5
NC2	63 ± 4.2	0.670	+0.42 ± 0.3	57 ± 1.2	52 ± 4	8.5 ± 0.7	8.6 ± 0.8
NC3	71 ± 3.9	0.571	+0.51 ± 0.2	64 ± 3.2	67 ± 6.2	9.5 ± 0.4	9.3 ± 0.7
NC4	76 ± 7.6	0.510	+0.63 ± 0.5	73.5 ± 2.5	72 ± 2.7	10 ± 0.7	9.8 ± 0.6
NC6	85 ± 8.5	0.318	+0.7 ± 0.4	91 ± 1.9	89.5 ± 1.2	11.5 ± 0.6	10.8 ± 0.5
NC7	216 ± 10.5	0.710	+0.9 ± 0.31	87 ± 3.4	89 ± 3.4	10.6 ± 0.3	9.7 ± 0.6
NC8	309 ± 14.6	0.720	+1.3 ± 0.21	90 ± 4.1	88 ± 1.2	10.2 ± 0.5	9.8 ± 0.3

icals are largely been implicated in nanomedicine and drug delivery due to considerable biological activities for safe and effective uses for the intended purpose.[18−23]

Ciprofloxacin (Figure 1B) is a fluoroquinolone antibiotic that has low solubility and permeability ensuring variable absorption and restricted bioavailability. It inhibits the DNA gyrase enzymes required for DNA replication. It is used against infections produced by both Gram-positive and negative bacteria of the respiratory tract, urinary tract, eye, and ear infection. It is also recommended for anthrax, salmonella infection, typhoid fever, gonorrhea, and joint infection.[24] The usual dose of ciprofloxacin is 500 mg twice a day. Encapsulating oleic acid mixed ciprofloxacin into nanoparticles can improve the drug, dissolution, absorption, bioavailability, and antimicrobial activity of the drug.[25]

Naringin (Figure 1C) is a derivative of Naringenin (aglycone) and belongs to flavonoids glycoside of the flavonone class mainly obtained from citrus fruits, lemon, grapes, beans, cherries, oregano, and orange.[25,26] It has multiple pharmacological actions of antioxidant, antimicrobial, antibiofilm, antitumor, antihypertensive, antidiabetic, antiviral, and tissue regeneration and modulated through distinguished signal pathways.[27,28] Naringin also modifies the drug absorption, distribution, and elimination process in intestinal tissues and increases the bioavailability of paclitaxel.[29] It has antimicrobial activity against *E. coli* and *S. aureus*.[30] A study by Dey et al., reported that naringin enhances ciprofloxacin antimicrobial efficacy against *P. aeruginosa* biofilm compared to alone treatment.[3] Naringin has low oral bioavailability and biodistribution, hence affecting the therapeutic aim. In the current study, the rationale toward the codelivery of CIP with their herbal counterpart NAR in a biocomposite system is besides the antimicrobial action of CIP; NAR increases oxidative stress in *E. coli* and *S. aureus* and causes reactive oxygen species formation. It leads to the damage of bacterial membranes and biofilm sensitization resulting in improved antimicrobial efficacy.[31] Therefore, the current study aimed to design and evaluate the codelivery of naringin and ciprofloxacin from the oleic acid lipid of carboxymethyl chitosan/alginate nanoparticles and evaluate the in vitro for drug release and investigate enhanced antimicrobial activity of CIP bearing NAR in comparison to CIP solo use against different bacterial strains, *E. coli*, and *S. aureus*.

RESULTS AND DISCUSSION

Optimization of the Nanosystem. Based on the preliminary investigation of the development of the CIP + NAR− CM−CS/SA−NPs composite system, the different formulation codes (NC1−NC8) of varying formulation compositions were designed. The CIP and NAR in a ratio of 1:5 were successfully encapsulated in the nanocomposite system with maximum entrapment efficiency of 91 ± 1.9 and 89.5 ± 1.2%, respectively. For solubilization and improved dissolution of drugs, a low drug to oleic acid ratio of (1:0.5) to a high drug to oleic acid ratio of (1:4) were tested precisely in vitro. Increasing oleic acid concentration increased drug entrapment due to higher solubilization. At an optimum ratio of drugs to oleic (1:2.5) corresponding to formulation NC6, the maximum solubilization of drugs was achieved. Toragall et al. prepared a hybrid carrier using oleic/chitosan/alginate and improved aqueous solubility and intracellular transport of hydrophobic drug lutein.[32] The increasing concentrations of CM−CS (0.5−3 mg/mL) and SA (0.25−2.0 mg/mL) were used in the formulation optimization process while keeping the same concentration of 0.15% tween 80. At the least concentration of 0.5 mg/mL of CM−CS and 0.25 mg/mL of SA; the particle size, PDI, and zeta potential was recorded 50 ± 2.6 nm; 0.507; and +0.3 ± 0.1 mV. While, the drug entrapment was observed less, i.e., 42 ± 2.7 and 39 ± 0.8% for CIP and NAR may be due to low polymer content that was unable to encapsulate the added amount of drugs; on the other hand, increasing their concentration, increased the particle size due to bulkiness of the particle. The % drug loading of CIP and NAR was measured to be 8.3 ± 0.6 and 8.4 ± 0.5%.

At the polymer concentration of CM−CS and SA of 2 and 1.5 mg/mL (NC6), the particle size of 85 ± 8.5 nm, PDI of 0.318, zeta potential of +0.7 ± 0.4 mV, and drug entrapment (CIP to NAR) of 91 ± 1.9 and 89.5 ± 1.2% were incurred, respectively. Further, at the same concentration % drug loading of CIP and NAR were measured 11.5 ± 0.6 and 10.8 ± 0.5%. The highest particle size of >300 nm was retrieved at a polymer concentration of 3 and 2.5 mg/mL of CM−CS and SA. The least particle size, low PDI (monodisperse), and high entrapment and loading were measured for formulation NC6. The detailed characterization results of formulations (NC1−NC8) are shown in Table 1. Ebrahimi et al. prepared NAR and Berberine loaded Chitosan/Alginate hydrogel composite of mean particle size and entrapment of Berberine and NAR were 594 nm; 51.6 ± 7.4% and 636 nm and 47.1 ± 5.8%.[33] The optimized nanoparticles composite system leveled to formulation code NC6 (CIP + NAR−CM−CS/AG−NPs) has comprised 100 mg of CIP, 20 mg of NAR, drugs to oleic ratio of 1:2.5 and tween 80 of 0.15%, CM−CS of 2 mg/mL, and SA of 1.5 g/mL, respectively. The optimized preparation was characterized in vitro for further investigation.

Physicochemical Characterization of the Nanosystem. The prepared optimized formulation showed a particle size of 85 ± 8.5 nm, PDI of 0.318, and ζ-potential of +0.7 ± 0.4 mV. The amount of drug safely encapsulated as drug entrapment and loading corresponding to CIP to NAR were 91 ± 1.9, and 89.5 ± 1.2; 11.5 ± 0.6 and 10.8 ± 0.5%, respectively. Further, the size

https://doi.org/10.1021/acsomega.3c08200
ACS Omega 2024, 9, 6845−6860

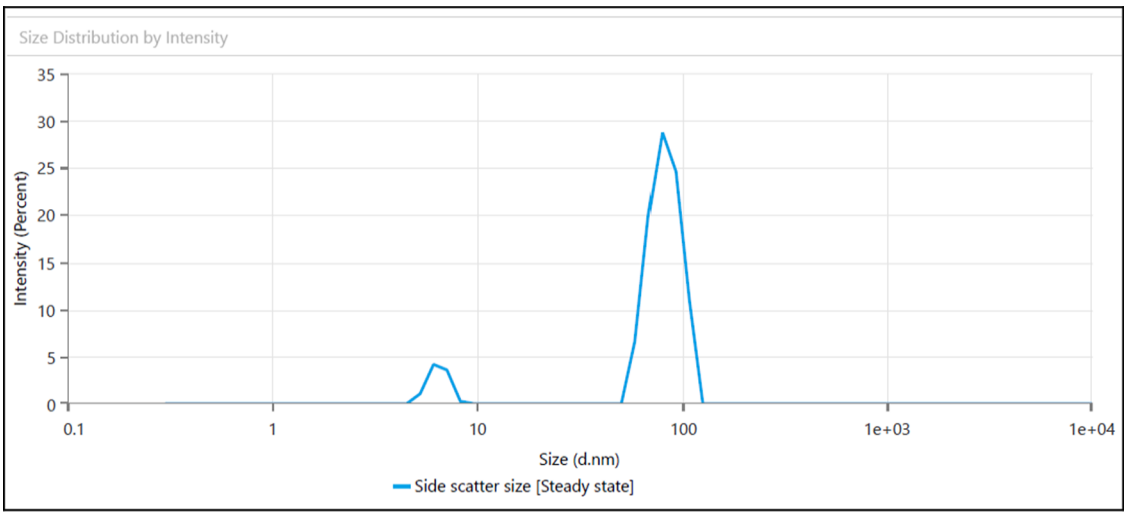

Figure 2. Particle size distribution by percentage intensity of CIP + NAR−CM−CS/AG−NPs.

distribution in the bulk of the formulation was highly consistent and unimodel. The homogeneity, uniformity, and single-phase size distribution of the nanodrug delivery system were also confirmed by low PDI. The chitosan molecules bear a positive surface charge due to the presence of NH_3+ ions. However, methyl carboxylation of chitosan reduces positive charge toward zero or negative. Here, the surface potential of CIP + NAR−CM−CS/AG−NPs was recorded as very less positive, indicating that the methyl carboxylation brings down the positive charge significantly due to the formation of carboxylate ion (CH_2COO^-). The balance in positive and negative surface charge over NPs due to NH_3+ and carboxylate ion (CH_2COO^-) contributed toward the stability and robustness of the system and impersonated the stability in the biological medium.[34] The particle size and their distribution and surface charge on NPs are shown in Figures 2 and 3. The particle size depiction by Malvern

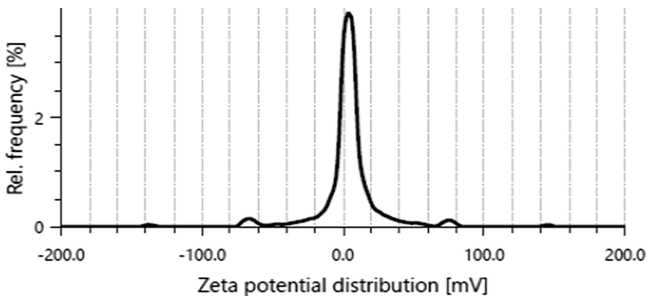

Figure 3. Particle surface charge representation of CIP + NAR−CM−CS/AG−NPs by the percentage relative frequency.

Zetasizer further elaborated by conducting TEM analysis expressed that the particle is stable, well dispersed, ordered, and coherent (Figure 4). The size of particles in the bulk preparation is obtained in nanometers.[35]

Differential Scanning Calorimetry. The physical state of therapeutics processed in the cargo for drug delivery is highly important to predict the fate of a biological system. DSC spectral peak mainly focuses on changes in the physical and chemical properties of the substances by evaporation (loss of water) and polymer decomposition and is characterized by exothermic or endothermic peaks. Differential thermal scanning is an important analytical tool used to determine the melting point

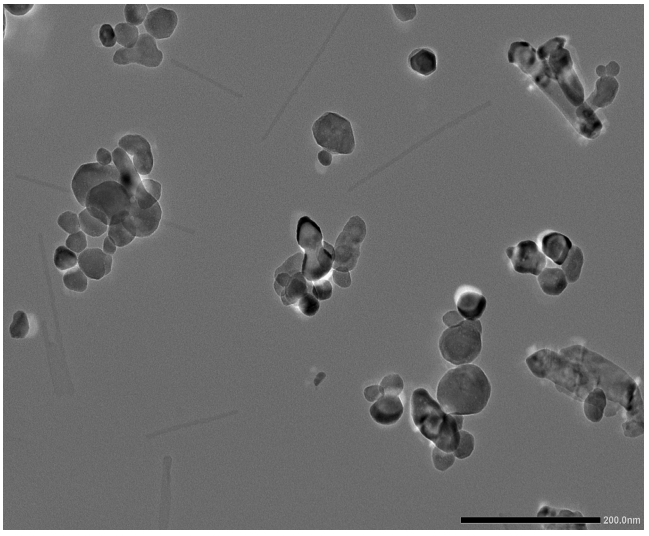

Figure 4. TEM image of CIP + NAR−CM−CS/AG−NPs.

of raw drugs and the physical state of a drug in a nanocarrier. The DSC thermogram of CIP, NAR, sodium alginate, carboxymethyl chitosan, and ciprofloxacin and naringin loaded-carboxymethyl chitosan/alginate nanoparticles are indicated in Figure 5A−F. The raw ciprofloxacin showed a peak of dehydration at 163.8 and 329.23 °C pointing to the crystalline melting of the drug during decomposition (Figure 5A). The melting endothermic peak of NAR obtained at 162.65 °C, and the thermogram showed at 106.69 °C (Figure 5B) was due to water loss.[36,37] A sharp endothermic spectrum of sodium alginate showed at 128.84 °C due to matrix water loss (Figure 5C). While carboxymethyl chitosan showed a sharp endothermic peak at 104.62 °C, a low endothermic peak at 168.51 °C, and a sharp endothermic peak at 283.8 °C due to different functional groups (Figure 5D).[38] Moreover, the physical mixture of formulating components showed melting peaks at 139.56, 166.88, and 239.93 °C (Figure 5E). The melting point of alginate in the formulation was slightly lowered and appeared at 75 °C and carboxymethyl chitosan was obtained at 100 °C (Figure 5F). However, no drug peak appeared on the formulation, demonstrating that the drugs have been encapsulated in the biopolymer composite.

https://doi.org/10.1021/acsomega.3c08200
ACS Omega 2024, 9, 6845−6860

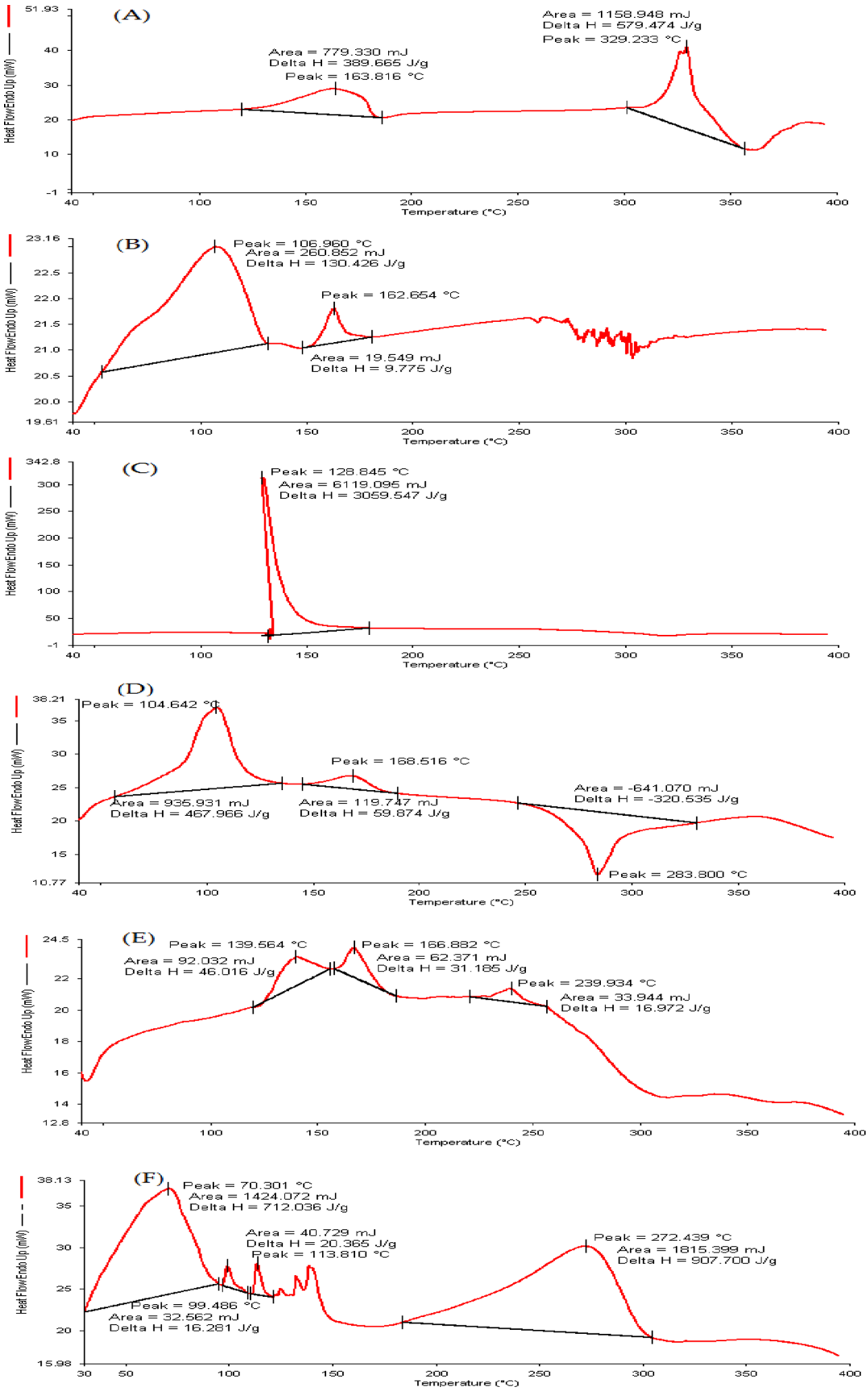

Figure 5. DSC curve. (A) ciprofloxacin, (B) naringin, (C) sodium alginate, (D) carboxymethyl chitosan, and (E) physical mixture; (F) formulation.

X-ray Diffraction Study. XRD was investigated to ensure the conversion of the crystalline structure of raw drugs into the molecular state of the drug encapsulated within a nanocarrier. The powder XRD of raw ciprofloxacin, Naringin, carboxymethyl

https://doi.org/10.1021/acsomega.3c08200
ACS Omega 2024, 9, 6845−6860

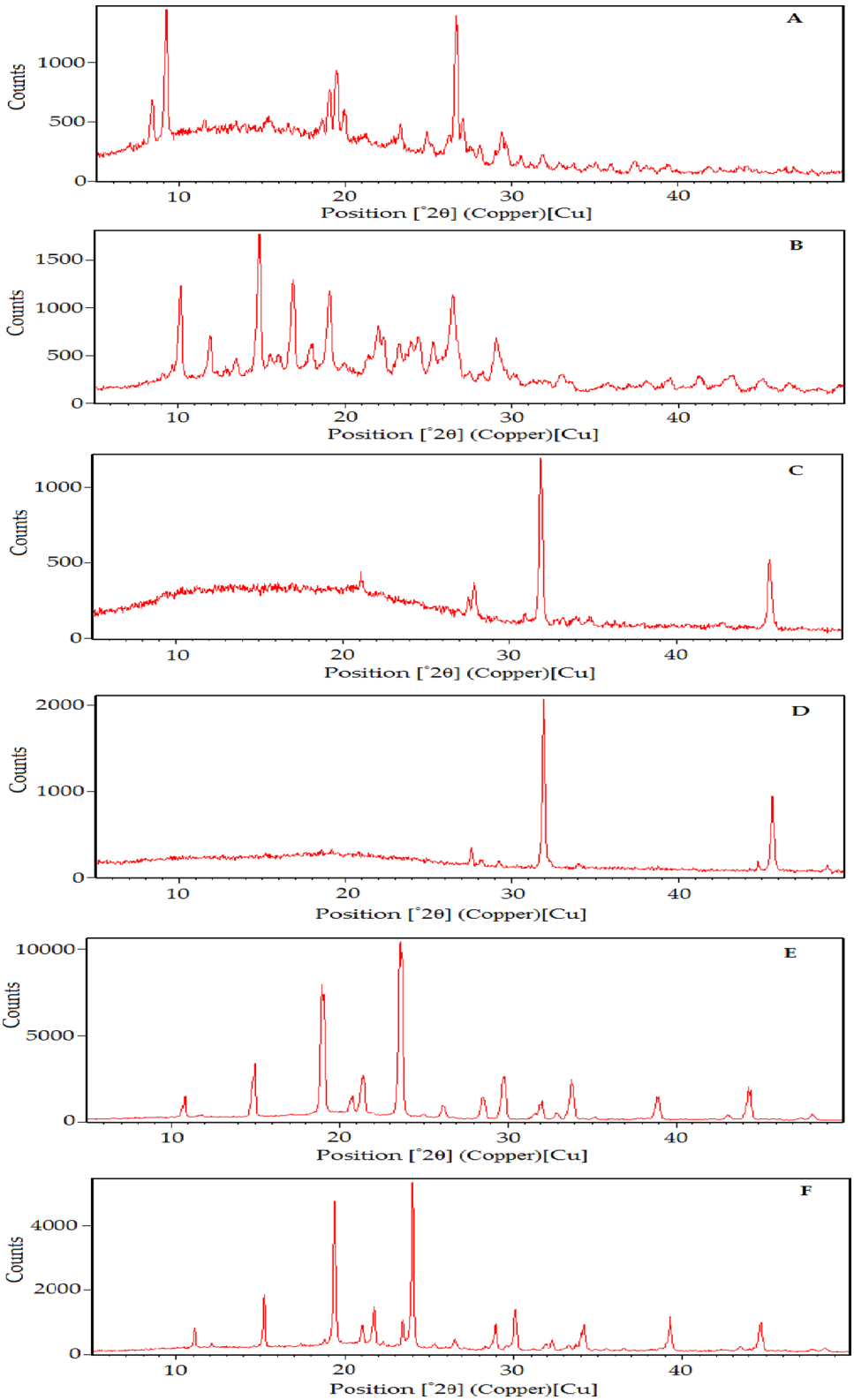

Figure 6. Powder XRD. (A) CIP, (B) NAR, (C) carboxymethyl chitosan, (D) sodium alginate, (E) oleic acid, and (F) CIP + NAR−CM−CS/AG−NPs.

chitosan, sodium alginate, oleic acid, and CIP and NAR-loaded oleic acid carboxymethyl chitosan/alginate nanoparticles are shown in Figure 6A−F. The specific diffraction pattern in the crystal structure of ciprofloxacin appeared at a sharp 2-theta of 9.1660 (area = 141.53), 19.4243 (area = 109.91), 26.6310 (area = 172.30), and 29.3833 (area = 77.73). Naringin shows specific crystal peaks at 2-theta of 9.8002 (area = 231.38); 10.1251 (area = 169.73; 11.9101 (area = 149.46), 13.4633 (area = 226.37), 14.8716 (area = 377.22), 16.8457 (area = 254.11), 17.9369 (area = 306.41), 19.0442 (area = 294.90), 24.0022 (area =

https://doi.org/10.1021/acsomega.3c08200
ACS Omega 2024, 9, 6845−6860

232.49), 26.4269 (area = 519.49), and 29.1146 (area = 341.64). Similarly, the sharp and intense peaks of CIP and NAR did not appear in the formulation; this may have been attributed to the molecular state of drugs encapsulated in the nanoparticles. Carboxymethyl chitosan and sodium alginate showed few intense peaks at a 2-theta of 31.8777 (area = 198.36), 45.5924 (area = 98.30), 31.8838 (area = 290.75), and 45.6148 (area = 152.48) due to some crystal structure. Oleic acid showed several sharp and intense peaks specifically at 2-theta of 14.8491 (area = 396.13), 17.2827 (area = 396.65), 18.9625 (area = 1414.84), 19.1032 (area = 360.38), 19.1032 (area = 360.38), 20.6959 (area = 674.09), 401.17 (area = 21.3480), 23.6015 (area = 1946.21), 23.7403 (area = 353.89), 28.5223 (area = 278.02), 29.7185 (area = 545.71), 33.7742 (area = 500.17), 38.8801 (area = 259.31), and 44.2859 (area = 421.89) probably due to high degree of crystalline structure. Surprisingly, XRD peaks appeared in a formulation at 2-theta angle of 15.2150 (area = 181.68), 17.4477 (area = 263.51), 19.3572 (area = 612.85), 21.0153 (area = 295.74), 23.9939 (area = 650.97), 34.0993 (area = 160.87), and 44.6138 (area = 188.08) was not from the CIP and NAR, rather from the external layer of oleic acid expressing that the drugs are well encapsulated within the polymeric matrix in the amorphous state.[39,40]

Drug Release from Formulation. The amounts of CIP and NAR released from nanoparticle and raw drug suspension were investigated at a fixed time, as shown in Figure 7. The time

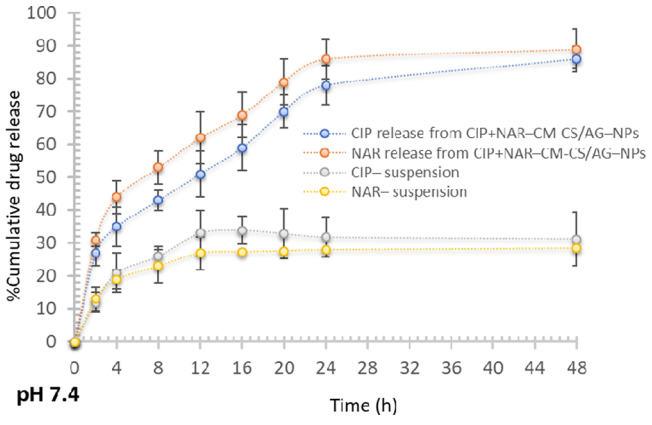

Figure 7. % Cumulative release of CIP and NAR from CIP + NAR−CM−CS/AG−NPs and their suspensions at phosphate buffer saline of pH 7.4.

point of drug release was noted at the beginning of the study and continuously monitored until the end of 48 h by appropriate sampling. Drug release was estimated in this period both from formulation and raw drug suspension. The CIP and NAR release from suspension was monitored for 48 h and at the end of the study maximum release was marked 31.26 ± 8.1 and 28.4 ± 5.6%, respectively. The slow and low release from raw drug suspension may be due to erratic solubility and dissolution behavior of unformatted drugs. Adversely, over the period of observation, the initial phase showed an abrupt release of 31 ± 1.6% NAR in 2 h from CIP + NAR−CM−CS/AG−NPs. The higher drug release on the initial phase at pH 7.4 (PBS) was noticed due to the solubilization of weakly held or surface-absorbed drug from the polymeric surface. Afterward, it experienced a drug liberation in a prolonged or sustained fashion for a period of 48 h in the medium i.e., 89 ± 6% in physiological pH 7.4. Similarly, the CIP release from CIP + NAR−CM−CS/AG−NPs was determined on samples collected at different intervals. The % drug release of CIP was estimated at 86 ± 4% from CIP + NAR−CM−CS/AG−NPs in the physiological medium of pH 7.4. The slow and sustained release of CIP was due to the strong bond formation (hydrogen or ionic interaction) between CIP and oleic acid and the carboxylic group from CIP further binds with positively charged carboxymethyl chitosan and thus overall, led to prolong the release rate from the nanoparticle composite. Similar trends of CIP release were observed from various nanocarrier and oleic acid alginate/chitosan nanosize particles quoted in the literature.[41−44] The carboxymethyl chitosan alginate composite nanoparticles hydrate in aqueous medium, resulting in swelling, erosion, and subsequent drug diffusion in the dissolution medium. Furthermore, drug liberation is sustained and prolonged from the alginate/carboxymethyl chitosan core depending upon the drug, polymer concentration, solubility, pH of the medium, and other physicochemical properties of the drug and cargo system.[45]

The percentage of drugs released from the nanocomposite system was fitted into the kinetic models to come across the mechanism of drug release from the drug-loaded composite system. The different models were adapted to the drug release likewise; Korsmeyer−Peppas, Higuchi model, Hixson−Crowell, first order, and zero order to discriminate the suitability of the model to fit. The kinetic data incurred from different models are shown in (Table 2). These models expressed varied release mechanisms from the lipidic/polymeric matrix.

Table 2. Kinetic Release Model Expressing Fitting Drug Release Data from CIP + NAR−CM−CS/AG−NPs

korsmeyer−peppas	higuchi	hixson crowell	first order	zero order	constants
0.951	0.906	0.891	0.705	0.838	regression coefficient $(R)^2$
0.31	0.56	0.68	0.50	0.71	exponent value, (n)

The regression value of the different models was determined and the highest value of it was assigned to the good fitted model. The Korsmeyer−Peppas model was chosen as the best-fitted model due to the high regression value of $R^2 = 0.951$. For other models, Higuchi, Hixson Crowell, zero order, and first-order regression values were $R^2 = 0.906$, $R^2 = 0.891$, $R^2 = 0.838$, and $R^2 = 0.705$, respectively. The mechanism of drug release from the lipidic/polymeric composite system favored diffusion of the Fickian type as illustrated by the exponent value (n) of 0.31 $(0.5 < n < 1)$. Further, controlled and sustained drug release conveyed through the matrix composite system triggered via hydration, swelling, and thereby diffusion, and then dissolved drug eroded from the lipid core−shell to the exterior layer in the surrounding environment. On the other hand, the drug release is also governed by adjacent biological medium pH, drug dose, physical and chemical behavior of the drug as well as polymer composite.[46,47]

Intestinal Permeation Study. The relative permeation profile of NAR and CIP from formulation was determined in a predefined interval of time. The amount of drug permeated from formulation CIP + NAR−CM−CS/AG−NPs and drug suspension were estimated across the goat intestine, which were obtained from a local slaughterhouse, cleaned, and washed with ringer solution clearing any type of foreign substances or cell debris. The rates of permeation as fluxes were estimated

https://doi.org/10.1021/acsomega.3c08200
ACS Omega 2024, 9, 6845−6860

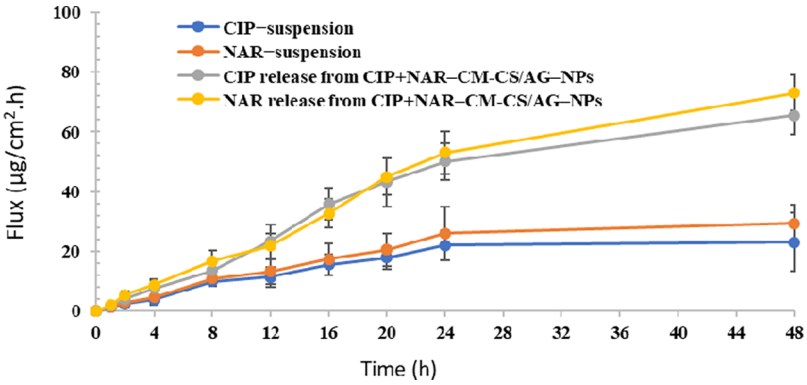

Figure 8. CIP and NAR permeation fluxes from CIP + NAR−MCS/AG−NPs and drug suspensions. Data are expressed as average ± SD (n = 3).

using UV−visible spectrophotometry of both CIP and NAR to concerning time shown in Figure 8. The permeation across the intestinal membrane expressed that the amounts of NAR and CIP permeated from the formulation CIP + NAR−CM−CS/AG−NPs were 65.43 ± 6.45 and 73 ± 6 $\mu g/cm^2$ h in 48 h. Similarly, unformulated NAR and CIP suspensions showed fluxes of 29.34 ± 6.3 and 23.1 ± 9.9 $\mu g/cm^2$ h at the same time. This may have been ascribed to the unformulated state of NAR and CIP in suspension. Further, the NAR and CIP permeation rate was significantly higher than that of the drug suspension ($p < 0.01$).

Intestinal absorption of drugs is greatly affected by mucoadhesive properties and mucosal cell interaction with the surface area of the nanocarrier. The positive surface potential of chitosan is due to bearing protonated amino group (NH_3^+) favoring mucosal drug transport via the nanobiointeraction of the oppositely charged mucosal layer. In addition, the adequate nano surface area of the chitosan alginate composite could assist in the permeation process through the intestinal epithelial junction.[48,49]

Hemocompatibility Assay. The blood compatibility assay of the developed preparation CIP + NAR−CM−CS/AG−NPs was examined for the compatibility of preparation with blood cells in the systemic circulation. A limited percentage <2% of RBC destruction is permitted and considered safe administration of formulation. The cell destruction is probably due to the cytotoxic nature of raw materials and polymers used in the preparation. The formation of instant protein covers around the NPs due to protein adsorption (protein corona) in blood circulation, and the resulting interaction with them may disfigure the geometry and original structure of NPs. The NPs in direct contact with cellular components may induce thrombosis or damage blood cells and release hemoglobin. The percentage of hemolysis of less than 2% recommended safer administration according to the ASTMF756-00 (2000) standard.[50] The use of natural biomaterial may be accounted as safe and compatible with the biological system.[51]

DPPH-Radical Scavenging Assay. 2,2-Diphenyl-1-picrylhydrazyl (DPPH) is a widely accepted and easily performed way of measuring antioxidant power, where it acts as a free radical. The antioxidant power of the biological compound NAR is widely explored with the DPPH assay for determining radical scavenging activity. The ability of the proton (H^+) donor of the antioxidant sample was estimated by discoloration of the organic solution of DPPH. The DPPH reagent produces a purple or violet color in methanol solution. The DPPH reagent in contact with antioxidant samples causes the color conversion to fade yellow or colorless. The antioxidant capacity of NAR from NAR−CM−CS/AG−NPs was determined to be 87.33 ± 4.3 versus 59 ± 6% by naïve NAR. The positive control BHT and blank nanocarrier showed 98.4 and 23.3 ± 8.65% of antioxidant capacity. The antioxidant activity of NAR from CIP + NAR−CM−CS/AG NPs did not alter in the presence of CIP and almost remains the same (Figure 9). The finding conveyed that

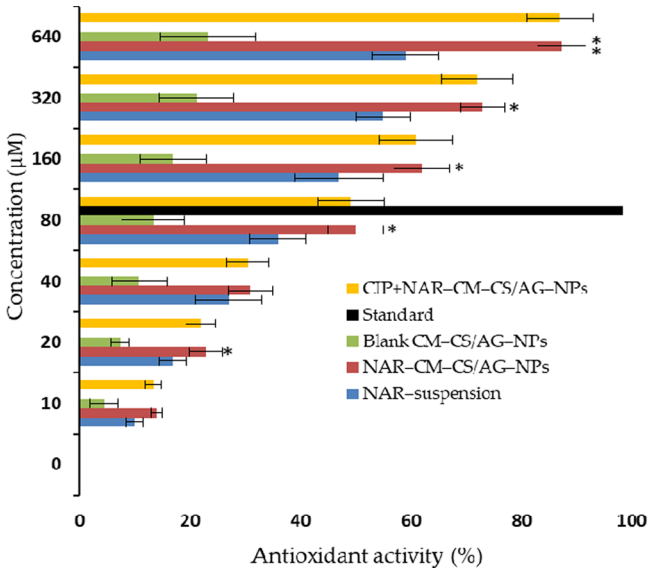

Figure 9. Antioxidant activity of NAR from NAR−CM−CS/AG−NPs by DPPH assay in comparison to the NAR suspension and blank CM−CS/AG NPs positive control: BHT was used as standard. The significant difference was considered when expressed *$p < 0.05$; **$p < 0.01$ (highly significant). Data expressed as average ± SD (n = 3).

the antioxidant properties of NAR were concentration-dependent. The result interpreted that NAR in the nanocarrier acts as an excellent antioxidant compared to naïve NAR showing the importance of nanotechnology-based processing of naïve NAR due to their successful entrapment in the polymeric core. This could be due to the enhanced dissolution of NAR trapped in the carrier and protected against harsh environmental conditions. Naïve NAR showed less antioxidant properties compared to NAR formulation due to its poorly dissolved state. The antioxidant capacity of formulated NAR is comparable to the current studies accounted for in the scientific literature.[51,52]

Nano-State Stability. The nanosize stability of the optimized formulation is shown in Figure 10A−D. The formulation stability was investigated for modification in the

https://doi.org/10.1021/acsomega.3c08200
ACS Omega 2024, 9, 6845−6860

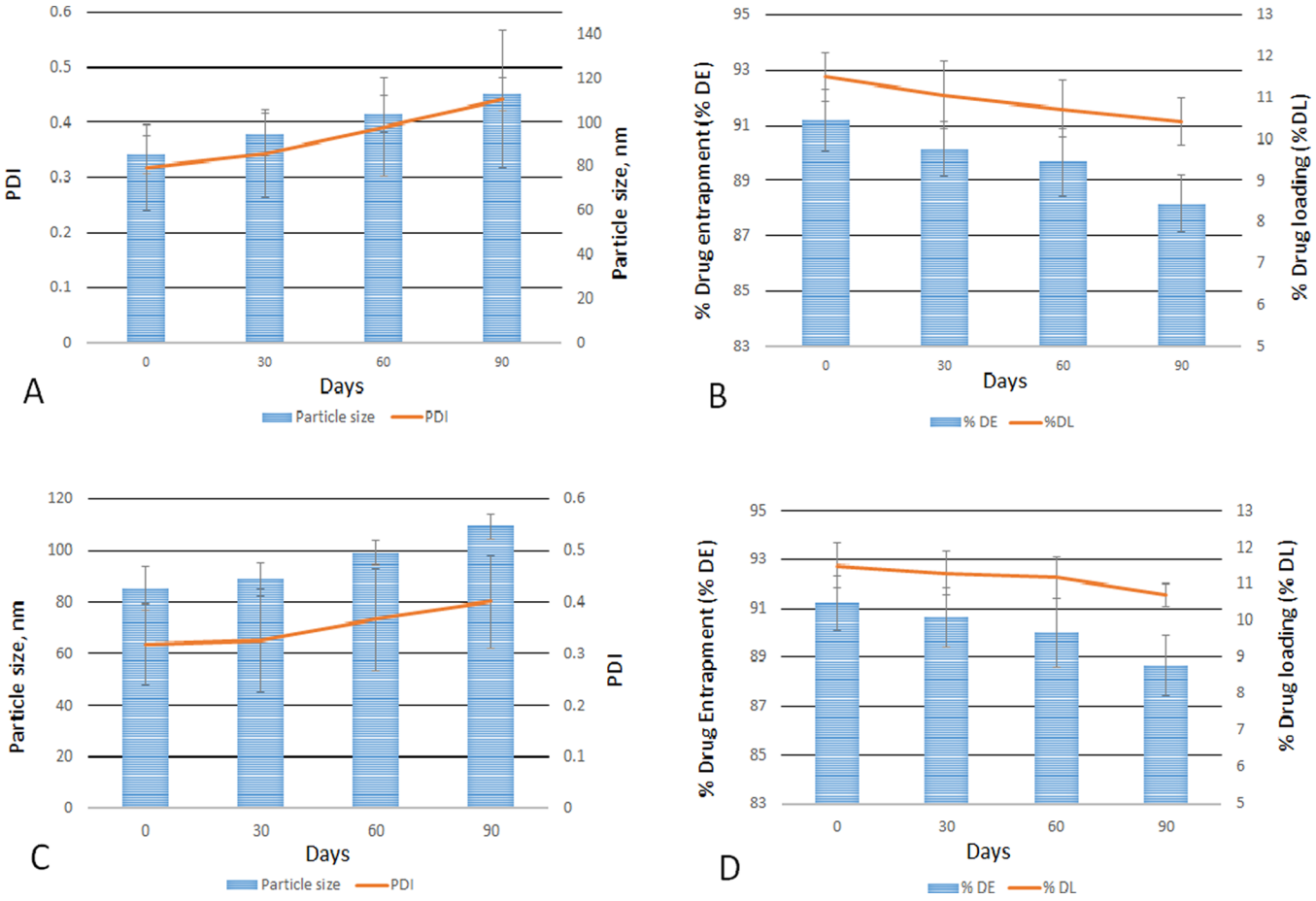

Figure 10. Evaluation of the nano-state stability of the developed formulation. The changes in the particle size, PDI, and % drug entrapment and drug loading of CIP + NAR−CM−CS/AG−NPs at room temperature 25 ± 2 °C (A and B) and at 5 ± 2 °C (refrigerated condition) (C and D). Data expressed as average ± SD (n = 3).

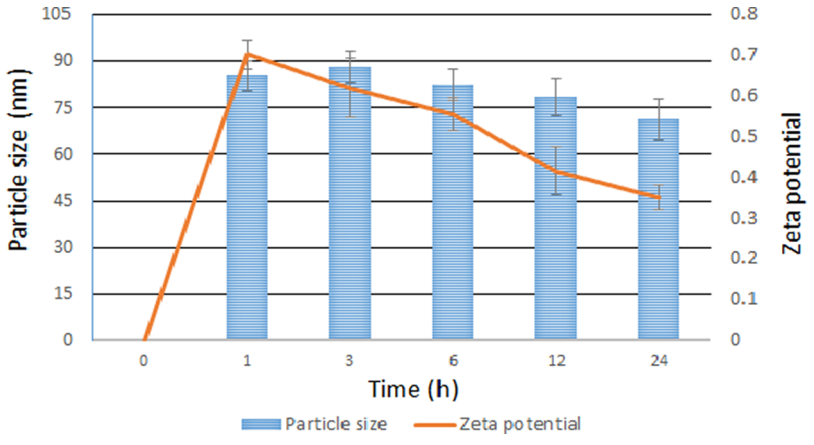

Figure 11. Physiochemical changes (particle size and surface charge) of the nanodrug delivery system in 5% FBS at nanobiointerface in biological milieu. Data expressed as average ± SD (n = 3).

physicochemical properties of the developed formulation for a defined period of 3 months. The changes were examined for particle size and their distribution, PDI, % drug entrapment, and % drug loading. A nonsignificant increase in particle size was noted probably due to the accumulation of particle mass of opposite charge particles ($p > 0.05$) in either room temperature or refrigerated conditions. A slight increase in PDI was also observed in the formulation due to particle assembly; despite this, the unimodal particle size distribution was unchanged. The change in the particle size, PDI, and size distribution did not alter the physicochemical properties of NPs and maintained their stability throughout the stability study. The % drug entrapment and % drug loading of NPs were also determined in this period, indicating a marginal fall in drug entrapment and drug loading efficiency. This may be ascribed to the fact that an aqueous medium may help in polymeric matrix wetting, hence the chances of drug leakage resulting in decreased drug loading and entrapment.[35]

https://doi.org/10.1021/acsomega.3c08200
ACS Omega 2024, 9, 6845−6860

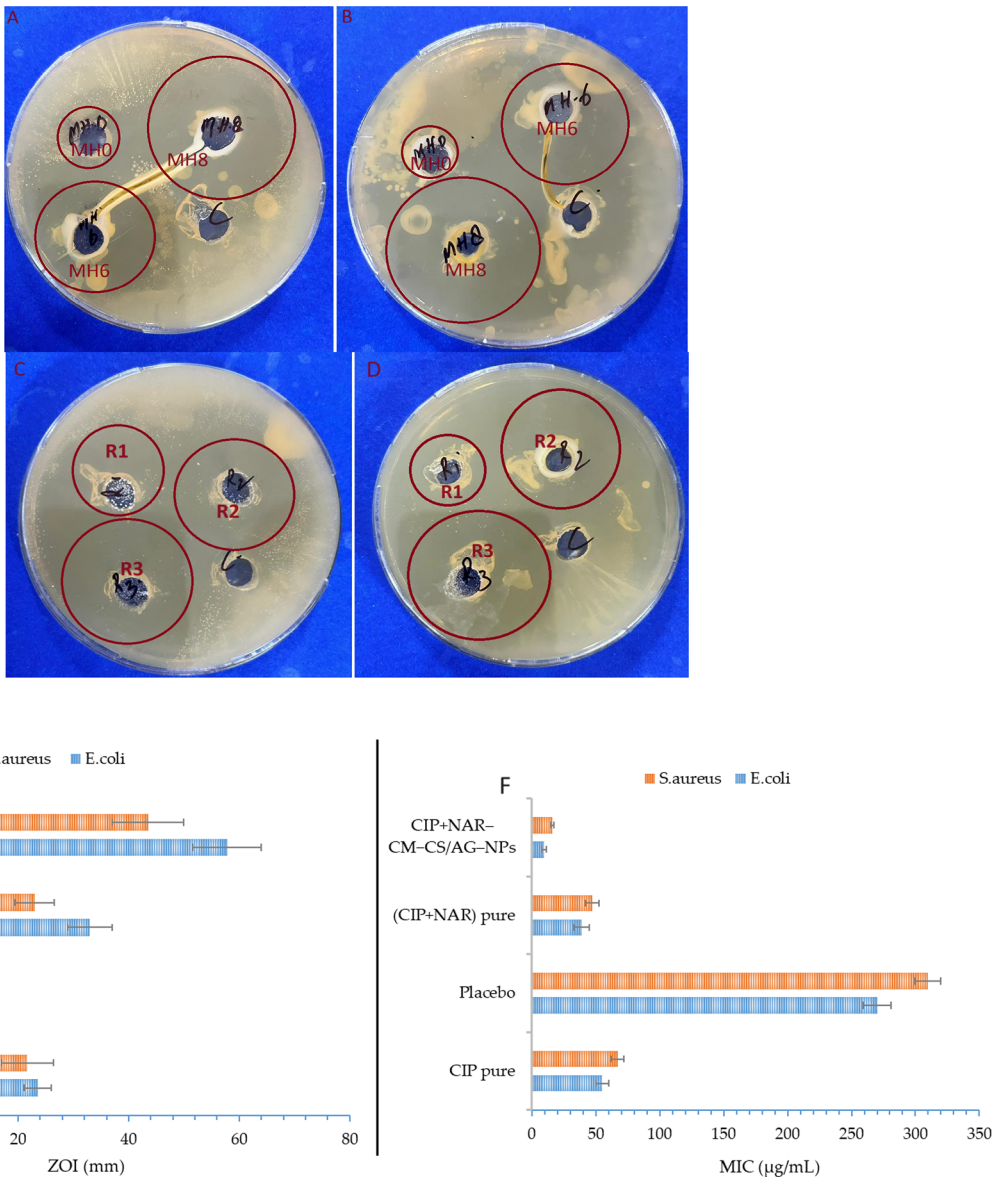

Figure 12. Antimicrobial experiments involving S. aureus (A, C), and *E. coli* (B, D) showed different ZOI (E) and MIC values (F) on groups: MH0 (Placebo); MH6−representing CIP pure; and MH8−representing CIP + NAR−CM−CS/AG−NPs formulation and; C−representing distilled water (control) (A, B). R1−representing CIP pure; R2−representing (CIP + NAR) pure; and R3−representing CIP + NAR−CM−CS/AG−NPs formulation (C, D). ZOI and MIC value of CIP + NAR−CM−CS/AG−NPs, (CIP + NAR) pure, placebo, and CIP pure (E, F). Data expressed as average ± SD (n = 3).

Table 3. MIC and ZOI of Formulation/Pure Drugs

	MIC (μg/mL)		ZOI (mm)	
formulation/pure drug	*E. coli*	*S. aureus*	*E. coli*	*S. aureus*
CIP pure	55 ± 4.4	67 ± 5	23.56 ± 2.4	21.67 ± 4.67
placebo	270 ± 11	310 ± 10	1.89 ± 0.69	1.46 ± 0.53
(CIP + NAR) pure	39 ± 6	47 ± 5.2	33 ± 4	26 ± 4.5
CIP + NAR−CM−CS/AG−NPs	9.4 ± 1.6	16 ± 0.5	57.8 ± 6.2	43.52 ± 6.4

Nanoparticle Stability in Fetal Bovine Serum (FBS). Serum stability of NP postincubation for 24 h is shown in Figure 11. Through this study, the authors came across to know the in vivo fate of NP and how it presents to the biological milieu. It was observed whether the in vitro prediction of their synthetic identity gets modified in vivo or they kept their original identity. Moreover, it was reported that increased absorbance of the sample over 3 h of the study clearly expressed that there was a layering of proteins around the NPs probably due to the interaction of macromolecules on to the NP surfaces or nanobiointeractions. The next observation focused on the impact of protein layering on to the NP surface that would have changed the inherent in vitro optimizing parameters of formulation such as physicochemical features of NPs like the particle size, size distribution, and surface potential. After 1 h of incubation, NPs had expressed an increased size, which led to an

https://doi.org/10.1021/acsomega.3c08200
ACS Omega 2024, 9, 6845−6860

overleap of the size observed at th end of 24 h. Overall, the increase or reduction in particle size in 24 h of incubation was not significantly different manifesting the nanosize stability at the nanobiointerface. A change of surface of NPs was reported from +0.4 to +1.4 mV throughout incubation indicating positive interaction with macromolecules in the biological medium.[53,54]

Antimicrobial Assay. The antimicrobial assay of the developed formulation in terms of zone of inhibition comparative to standard and control was determined, as shown in Figure 12A−D. The minimum inhibitory concentration (MIC) value of CIP + NAR−CM−CS/AG−NPs, (CIP + NAR) pure, and CIP pure was calculated for the chosen microbe (*S. aureus* and *E. coli*) as shown in Table 3 and Figure 12E,F to clarify the difference in activity. It was observed a notable growth suppression on both the strain of *S. aureus* and *E. coli* under study. The bacterial growth regression in terms of zone of inhibition measured were 21.67 ± 4.67, 1.46 ± 0.53, 26 ± 4.5, and 43.52 ± 6.4 mm for CIP pure, placebo, (CIP + NAR) pure, and in combination as CIP + NAR−CM−CS/AG−NPs formulation against *S. aureus*. In parallel to these, the zone of inhibition notably measured 23.56 ± 2.4, 1.89 ± 0.69, 33 ± 4, and 57.8 ± 6.2 mm for CIP pure, placebo, (CIP + NAR) pure, and in combination as CIP + NAR−CM−CS/AG−NPs for the strain *E. coli*. The tested efficacy of CIP with the occurrence of NAR in the formulation significantly enhanced in suppressing bacterial growth due to a higher zone of inhibition (ZOI). Further, the inhibition zone was higher for *E. coli*, however, growth suppression was not significantly different as compared to *S. aureus*. Moreover, the MIC values of pure CIP, (CIP + NAR) pure, and CIP + NAR−MCS/AG−NPs were estimated against both strains. The MIC values of the CIP pure, (CIP + NAR) pure and formulation CIP + NAR−CM−CS/AG−NPs were determined 55 ± 4.4, 39 ± 6, and 9.4 ± 1.6 μg/mL for *E. coli*. The drastic enhancement in antibacterial efficacy by CIP and NAR together due to encapsulation in nanocarrier. The drug encapsulation inside the polymeric core prominently improved the drug dissolution and their availability to the target, resulting in improved efficacy. Similarly, the MIC value of CIP pure, (CIP + NAR) pure and formulation CIP + NAR−CM−CS/AG−NPs were determined 67 ± 5.0, 47 ± 5.2 and 16 ± 0.5 μg/mL in case of *S. aureus*. The MIC values of CIP and NAR in nanoparticles were significantly different ($p < 0.01$) from those of CIP pure and (CIP + NAR) pure, exhibiting that drug-loaded nanoparticles showed greater antimicrobial activity. The combination index for codelivery of CIP and NAR from CIP + NAR−CM−CS/AG−NPs was investigated, which ascertained the enhanced effect of CIP in the presence of NAR, i.e., a synergistic effect where the CI value of drugs calculated 0.28 for *E. coli* and 0.48 for *S. aureus*, and it was affirmed by the Chou−Talalay method.[55]

The antibiotic release mediated from the nanocarrier for intracellular delivery may be challenging due to nanobiointeraction with biological membranes. However, nanoparticles showed improved delivery to the cell, organs, and tissue due to optimized and tuned surface geometry. The current antimicrobial study results outcomes are comparable to the previous work by Imam and associates.[52]

Tijani Isa and associates designed Ciprofloxacin loaded Aragonite NP and tested the in vitro antibacterial activity against Salmonella Typhi. The developed formulation showed the average zone of inhibition 18.6 ± 0.5 mm parallel to 11.7 ± 0.9 mm by ciprofloxacin pure.[39] Ciprofloxacin HCL-loaded chitosan nanoparticles were fabricated by Soliman et al.[56] using the ionic gelation technique. The formulation was optimized by a Box-Behnken design. Different parameters optimized under the study showed the quadratic impact of input variables on formulation processing. The optimized NPs were effective at low concentrations of CIP-loaded nanoparticles and the inhibition zone of bacteria was not shown.[56]

Sobhani et al. developed CIP-encapsulated chitosan nanoparticles by the ionotropic gelation method. The impact of different mass ratios of chitosan was well studied in drug encapsulation and other physicochemical parameters of the formulation. The antimicrobial activity of formulation was measured in terms of MIC value and the results exhibited nanoparticles containing CIP was shown to be a 50% lower MIC value compared to naked CIP against *E. coli* and *S. aureus*. The study concluded that CIP at a low dose in nanocarrier could be effective against bacterial infection.[57]

The combination of CIP and NAR in a chitosan-alginate nanoparticle was not reported earlier in the literature. The results clearly showed that CIP in combination with NAR has shown improved antibacterial activity against the chosen microbial strain.

Imam et al. prepared an oral NAR hybrid nanocarrier for antibacterial activity and antioxidant activity using lipid and chitosan and optimized formulation by statistical design. The optimized formulation expressed encapsulation of 83.5 ± 2.1% and particle size 85 ± 8.5 nm. The drug release from the nanocarrier was noted as 89.62 ± 4.54%. They noticed improved antimicrobial activity against *E. coli* with respect to *S. aureus* and concluded that hybrid nanoparticles could be an alternate therapeutic mode in antimicrobial therapy.[49,52]

The aforementioned antimicrobial observation illustrated that the antibacterial activity of CIP enhanced in the presence of the NAR when entrapped in chitosan alginate nanoparticles. This may be due to the drug-carrying potential of the nanocarrier to the target site and also protecting against harsh biological environments. The other reason could be the destabilizing impact on the cell wall resulting in higher penetration and permeation onto the microbial in turn leads to higher killing of microbes.[58]

CONCLUSIONS

The current study successfully produced a dual drug-loaded lipid core carboxymethyl chitosan/alginate NP for improved microbial treatment. The optimized formulation CIP + NAR−CM−CS/AG−NPs was extensively characterized in vitro and assessed for different parameters including intestinal permeation flux. The CIP and NAR release from the nanocarrier showed sustained release behavior after the initial drug eruption. The homogeneous and consistent size of nanoparticles obtained through Zetasizer analysis represents stable; and robust preparation. The particle size uniformity, shape, and size distribution, and their segregates were further ensured in the formulation by electron micrographic analysis. The polymeric/lipid matrix showed controlled drug release except in the beginning phase in the conterminous environment mediated by diffusion and exhibited a higher release in pH 7.4 for the intended time. Among the studied kinetic models, the Korsmeyer−Peppas was shown good fit for the model due to its high regression coefficient (R^2 = 0.951) and exhibiting Fickian diffusion. Moreover, DSC and spectral XRD analysis clearly expressed that the formulating components and drug were compatible and stable in the formulation. The high permeation flux of NAR and CIP from CIP + NAR−CM−CS/

https://doi.org/10.1021/acsomega.3c08200
ACS Omega 2024, 9, 6845−6860

AG−NPs relative to drug suspensions was observed from the permeation diffusion study. The developed biocomposite system illustrates serum stability in 24 h of incubation time which is paramount in nanobio stability in vivo. The antimicrobial assay of formulation revealed anticipated outcomes in reducing significant bacterial growth compared to the solo antibiotic treatment. To the end, the developed NAR and CIP entrapped in oleic acid carboxymethyl chitosan/alginate NPs composite improved the antimicrobial properties of CIP in combination with NAR. The developed nanoparticle composite bearing NAR and CIP could be an option in the clinical management of infection.

MATERIALS AND METHODS

Reagents. Carboxymethyl chitosan (Low M_w, 50−190 kDa, 90% deacetylation) obtained from Himedia Mumbai, India, sodium alginate (M_w 75−100 kDa). TCI Chemicals Pvt. Ltd. India, provided ciprofloxacin and naringin. Every chemical, solvents, and reagent used in this study were of high pure analytical standard.

Formulation and Optimization of the Composite System. The formulation was developed using a nonsolvent ionic gelation technique. In the meanwhile, in the development process, CM−CS bearing a positive surface charge was allowed to dissolve in acetic acid and SA was made to solubilize in an aqueous solvent. The different ratios of drugs (CIP: NAR) were dissolved in different ratios of drug to oleic acid and then transferred to a CM−CS solution. Finally, the SA solution was added to the drug-loaded composite system, sonicated, and centrifuged. The effect of process variables was studied in experimental outcomes of physiochemical properties of prepared nanoparticle composite including the particle size, surface charge, drug entrapment, and drug release. The experimental layout and formulation composition of the biocomposite system are enclosed in Table 4.

Table 4. Strategic Formula Composition for the Fabrication of the CIP + NAR− CM−CS/SA−NP Composite System

formulas code	NAR:CIP ratio	drug to oleic acid ratio	tween 80, %	CM−CS, mg/mL	SA, mg/mL
NC1	1:1	1:0.5	0.15	0.5	0.25
NC2	1:2	1:1	0.15	1.0	0.5
NC3	1:3	1:1.5	0.15	1.5	0.75
NC4	1:4	1:2	0.15	1.75	1.0
NC6	1:5	1:2.5	0.15	2.0	1.5
NC7	1:6	1:3	0.15	2.50	2.0
NC8	1:7	1:4	0.15	3.0	2.5

Fabrication of Ciprofloxacin (CIP)- and Naringin (NAR)-Loaded Carboxymethyl Chitosan (CM−CS)-Sodium Alginate (SA) Nanoparticles (CIP + NAR− CM−CS/SA−NPs) Composite Using the Nonsolvent Ionic Gelation Technique. The CIP + NAR−CM−CS/SA−NPs were designed and fabricated by the nonsolvent ionic gelation technique applying SA and CS as per Toragall et al., with modification.[59] First, 2 mg/mL CM−CS having a positive charge surface was dissolved in 0.1% acetic acid, and 1.5 mg/mL SA with a negative charge surface was dissolved in deionized water. Second, 100 mg of CIP and 20 mg of NAR both were dissolved in a 1:2.5 ratio of oleic acid and then added to CM−CS solution along with the addition of tween 80 (0.15%) and magnetically stirred (REMI CM-101 plus, India) for 1 h. Third, SA solution was injected as fine drops into the mixture of CS−CIP + NAR/oleic acid/Tween 80, and sonicated for 10 min, with probe sonicator (PCI, Mumbai, India) at 80 Hz at an amplitude of 80% under ice-bath, drug-loaded nanocarrier separated using centrifugation, dried, and lyophilized.

Characterization. *Particle Size Measurement.* A Zetasizer (Hitachi, H-7500) was used for investigating the particle size in the bulk of the nanosize formulation. Before the analysis of the particle size, the formulation was 50-fold diluted in deionized water, and after vortexing, the sample was observed.

Entrapment Efficiency (EE). The amount of ciprofloxacin and naringin entrapped in the nanocarrier was determined by the high-speed centrifugation method. After the centrifuge, the sample was withdrawn, the aliquot was removed with a micropipet, and then, the ciprofloxacin and Naringin content was estimated by using a UV−visible spectrophotometer. % EE was estimated by applying the below mentioned formula:

$$\%\ \mathrm{EE} = \frac{\text{Total drug dose} - \text{Supernatant drug}}{\text{Total drug dose}} \times 100 \quad (1)$$

Drug Loading. During the preparation of NPs, the quantity of drug entrapped per unit NPs weight expressed the drug loading. It was estimated by centrifugation technique using 2 mL prepared NPs and then drug concentration remained unentrapped as estimated using a UV−spectrophotometer. % DL was calculated using the below mentioned formula:

$$\%\ \mathrm{DL} = \frac{\text{Total drug encapsulated in NPs}}{\text{Total weight of NPs}} \times 100 \quad (2)$$

Differential Thermal Scanning (DSC). The DSC apparatus (Pyris 4 DSC, PerkinElmer, Waltham, USA) was employed to measure the precise melting peak of Ciprofloxacin, Naringin, and various excipients used in the developing formulation to generate the DSC thermogram. To assess the thermal scan, the DSC aluminum crucible was loaded with a 3.5 mg sample, a reference standard aluminum pan was kept empty, and then, the system kept on heating uniformly starting from 40 to 400 °C at a pace of 10 °C/min in a dry nitrogen gas environment.[23]

X-ray Diffraction Study. Powder XRD of ciprofloxacin, naringin, oleic acid, and other excipients were carried out to analyze the crystal morphs or physical state of drugs, components, and in the formulation. The samples were scanned under 2θ range of 10−50 °C in light radiation of wavelength 1.5406 Å, voltage 40 kV, current 30 mA, scan speed 8°/min using simple phase analysis (Rigaku Ultima IV) with scintillation counter as a detector.

Drug Release Study. Ciprofloxacin and naringin release from formulation CIP + NAR−CM−CS/SA−NPs was studied and compared to the release rate from raw drug suspension in phosphate buffer saline (PBS) pH 7.4 using a dialysis membrane. The precise noted quantity of formulation containing CIP and NAR and drugs suspension were separately loaded in a dialysis membrane previously filled with 150 mL of buffer solution and placed in a buffer solution of temperature upheld at 37 ± 0.5 °C, and the solution consistently stirred at 100 rpm.[53] At different time points (0, 2, 4, 8, 12, 16, 20, 24, and 48 h), 1 mL of sampling was done, and the same volume was replaced to keep the sink condition. The samples removed at each time point were investigated for CIP and NAR concentration using a UV spectrophotometer at 276, and 285 nm % cumulative release was calculated. The various kinetic models were studied after fitting the % drug release. The model of good fit was assessed by a simple graphical method, and a drug

https://doi.org/10.1021/acsomega.3c08200
ACS Omega 2024, 9, 6845−6860

release mechanism from a polymeric carrier was suggested. Moreover, the release mechanism from the polymeric carrier system was proposed based on the obtained value of the model exponent value (n). When the exponent value was $n \leq 0.5$ the released mechanism followed Fickian diffusion, while with the exponent value of $0.5 < n < 1$, the drug release mechanism from the polymer matrix pertains to anomalous non-Fickian diffusion. If the exponent value is equal to 1, that refers to a non-Fickian case II (relaxational) transport or zero-order kinetic model, and, if $n > 1$ it equates to a super case II transport.[60]

Drug Release Data Fitting to Kinetic Models. Many kinetic models are useful to discriminate the fitting good model to the drug release data comprising Korsmeyer−Peppas, Higuchi, Hixson Crowell, first-order, and zero-order. These models well explained the release mechanism from the polymeric/lipid matrix composite.[61]

Gut Intestinal Drug Permeation. The freshly prepared membrane was loaded with 10 mg of formulation and a parallel quantity of drug suspension, and then, the ends were closed. The membranes were immersed into a buffer solution of pH 7.4 in a beaker maintained at 37 ± 0.5 °C. The quantity of drug permeated at a defined interval was calculated by withdrawing the samples, and the same quantity of the medium was replaced with the beaker. The drug quantity permeated at a fixed time was estimated using a UV−visible spectrophotometer at λmax of 285 and 276 nm.

Hemolysis Assay. The hemolysis assay was carried out to investigate the compatibility of the developed formulation with blood. The preparation was diluted and well mixed with supernatant in a ratio of 2:1 and incubated for one hour at body temperature. The supernatant of citrated blood was obtained after centrifuging at 3,500 rpm for 10 min. Further, a part of the whole blood was mixed and added to deionized water that caused 100% hemolysis, which was noted as a positive control, and another part of the same was incubated with normal saline in a ratio of 1:1, which was noted as a negative control. After the sample was incubated, it was centrifuged at 3500 rpm for 10 min. The aliquot obtained thereafter centrifugation was taken and released hemoglobin due to the destruction of RBC was measured at 540 nm using a UV−visible spectrophotometer and absorbance set down. The percentage hemolysis or hemolytic index was determined by the formulation and other samples.[62]

$$\% \text{ Hemolysis} = \frac{\text{Abs TS} - \text{Abs NC}}{\text{Abs PC} - \text{Abs NC}} \times 100 \quad (3)$$

where "Abs TS" indicates the absorbance measured for the test sample; "Abs NC" indicates the absorbance of negative control; "Abs PC" indicates the absorbance measured for positive control.

DPPH Radical Scavenging Power of Naringin. The DPPH assay was carried out to investigate the suppression of free radical properties of NAR−CM−CS/SA−NPs and NAR− suspension as per modified procedure by Gabriele et al.[63] For the preparation of stock solution, 10 mg of NAR−CM−CS/SA−NPs, CIP + NAR−CM−CS/SA−NPs, and NAR− suspension was transferred into a volumetric flask, leveled stock solution formulation, and drug suspension. Dilutions of each stock solution were prepared ranging from 10 to 640 μM. The DPPH reagent of 0.03% w/v was prepared in ethanol and 100 μL was mixed with 1 mL of sample in the specified range. The mixer was vortexed and this complete set of samples was kept in a dark place at ambient temperature for 1 h. Thereafter, the complete samples were examined for color change owing to the reaction between the DPPH reagent and sample, i.e., violet to colorless. The maximum change in violet color to colorless suggests the better antioxidant capacity of the sample. Ethanol was used as a blank. Now, the complete samples were estimated by UV−visible spectroscopy at a specific wavelength of 517 nm using butylated hydroxytoluene (BHT) as the reference standard for comparing the antioxidant capacity. The antioxidant capacity of Naringin as percentage inhibition was plotted versus concentration. The IC50 was determined by data interpolation and compared with standard. The antioxidant capacity was determined using a formula.

$$\% \text{ DPPH radical inhibition} = \frac{A_0 - A}{A_0} \times 100 \quad (4)$$

where A_0 is blank sample absorbance; A sample absorbance.

Stability Study. The formulation stability was carried out as per guidelines of the International Conference on Harmonization to inspect the change in the physicochemical features of the final formulation in three months.

Serum Stability of NPs. The freshly prepared sample weighing 5 mg was transferred to an alkaline buffer, pH 7.4. Then, it was incubated with 5% FBS in equal concentrations of both formulation and serum at ambient temperature to investigate the layering of serum functional proteins over the NP surface. Moreover, the mixture was incubated at ambient temperature in a bath incubator for 24 h. The average diameter and surface charge of NPs in contact with serum were measured at different intervals of 1, 3, 6, 12, and 24 h. At predetermined points of time 1, 3, 6, 12, and 24 h, the sample was scanned using ultraviolet spectroscopy to trace out the position of λ_{max} of the active compound in the mixture with respect to the incubation time.

Antimicrobial Assay and Determination of the Combination Index (CI). The antimicrobial assays of CIP pure, CIP + NAR pure, and CIP + NAR−CM−CS/SA−NPs and control were performed employing the cup plate agar diffusion method. Briefly, CIP + NAR−CM−CS/SA−NPs bearing an equivalent amount of CIP and NAR as in pure drug preparation (15 μg/mL) were used in this study. For executing the antimicrobial activity, 10^6 cfu/mL each of *S. aureus* and *E. coli* were transferred to an agar medium in the Petri plate and allowed to solidify them. The agar medium was transferred to a Petri plate under strict provision of aseptic condition. Four wells were created into each Petri plate using a 5.5 mm sterile cork borer followed by the addition of 100 μL of formulation MH8 (CIP + NAR−CM−CS/SA−NPs), MH0 (placebo), MH6 (CIP pure) and C (sterile water) as control which is expressed in Figure 12A,B. Similarly, another plate received the same quantity of formulation CIP + NAR−CM−CS/AG−NPs (R3), (CIP + NAR) pure (R2), and CIP pure (R1) as shown in Figure 12C,D. The formulation and other solutions were allowed to diffuse in preincubation time of 1 h at ambient temperature, thereafter, plates were incubated for 1 day. After completing 24 h in the incubator plates were taken out, the zone of inhibition of each explored specimen was precisely measured, and results were compared statistically. The minimum inhibitory concentration (MIC) and zone of inhibition (ZOI) of pure drugs and drugs in the formulation were also determined.[52] The enhanced antimicrobial effect of CIP combining NAR as codelivery was measured in terms of combination index. It was calculated based on the MIC concentration of drugs achieved in an antimicrobial assay. The additive combination, synergistic, and antagonistic effects were

https://doi.org/10.1021/acsomega.3c08200
ACS Omega 2024, 9, 6845−6860

noted when (CI = 1), (CI < 1), and (CI > 1). The CI value was estimated using the following equation:

$$\mathrm{CI} = \frac{\mathrm{MIC}(A+B)}{\mathrm{MIC}(A)} + \frac{\mathrm{MIC}(A+B)}{\mathrm{MIC}(B)} \quad (5)$$

where MIC(A), MIC(B), and MIC($A + B$) expressed the MIC value of CIP, NAR, and a combination of CIP + NAR obtained in the antimicrobial assay.

One-way analysis of variance (ANOVA) was executed followed by Tukey−Kramer analysis was employed for statistical differences in groups using GraphPad Prism version 7. The data were analyzed as mean ± standard deviation ($n = 3$). Differences statistically between groups consider $p < 0.05$.

AUTHOR INFORMATION

Corresponding Authors

Md Habban Akhter − *Faculty of Pharmacy, DIT University, Dehradun 248001, India;* orcid.org/0000-0001-6278-0370; Email: habban.akhter@dituniversity.edu.in

Habibullah Khalilullah − *Department of Pharmaceutical Chemistry and Pharmacognosy, Unaizah College of Pharmacy, Qassim University, Unaizah 51911, Saudi Arabia;* Email: h.abdulaziz@qu.edu.sa

Authors

Tahani M. Almeleebia − *Department of Clinical Pharmacy, College of Pharmacy, King Khalid University, Abha 61421, Saudi Arabia*

Mohammad Akhlaquer Rahman − *Department of Pharmaceutics and Industrial Pharmacy, College of Pharmacy, Taif University, Taif 21974, Saudi Arabia*

Sarfaraz Ahmad − *Department of Clinical Pharmacy, College of Pharmacy, Jazan University, Jazan 114, Saudi Arabia*

Nawazish Alam − *Department of Clinical Pharmacy, College of Pharmacy, Jazan University, Jazan 114, Saudi Arabia*

Md Sajid Ali − *Department of Pharmaceutics, College of Pharmacy, Jazan University, Jazan 45142, Saudi Arabia*

Gyas Khan − *Department of Pharmacology, College of Pharmacy, Jazan University, Jazan 45142, Saudi Arabia*

Ibrahim Mufadhi M. Alanazi − *Department of Pharmacology and Toxicology, Faculty of Medicine, Umm Al-Qura University, Makkah 21421, Saudi Arabia*

Naiyer Shahzad − *Department of Pharmacology and Toxicology, Faculty of Medicine, Umm Al-Qura University, Makkah 21421, Saudi Arabia*

Amnah Alalmaie − *Department of Pharmaceutics, College of Pharmacy, King Khalid University, Abha 61421, Saudi Arabia*

Complete contact information is available at: https://pubs.acs.org/10.1021/acsomega.3c08200

Author Contributions

T.M.A. and M.H.A. contributed to conceptualization; T.M.A., M.H.A., and M.A.R. contributed to data curation; M.H.A. and S.A. contributed to formal analysis; H.K. and T.M.A. contributed to funding acquisition; T.M.A., A.A., and M.H.A. contributed to investigation; M.H.A., N.A., and M.S.A. contributed to methodology; M.H.A. and G.K. contributed to project administration. S.A., N.A., I.M.M.A., and H.K. contributed to resources; M.H.A., N.S., and M.A.R. contributed to software; T.M.A., I.M.M.A., and M.H.A contributed to supervision; N.A., N.S., A.A., and M.S.A. contributed to validation; G.K., N.S., I.M.M.A., and S.A. contributed to visualization; M.H.A. contributed to writing—original draft; and T.M.A., H.K., A.A., and M.S.A. contributed to writing—review and editing. All authors have read and agreed to the published version of the manuscript.

Notes

The authors declare no competing financial interest.

ACKNOWLEDGMENTS

The authors express their gratitude to the Deanship of Scientific Research at King Khalid University for funding this work through the Large Research Group Project under grant number R.G.P.02/535/44.

REFERENCES

(1) Chawla, M.; Verma, J.; Gupta, R.; Das, B. Antibiotic Potentiators Against Multidrug-Resistant Bacteria: Discovery, Development, and Clinical Relevance. *Front. Microbiol.* **2022**, *13*, 1−19.

(2) Vaou, N.; Stavropoulou, E.; Voidarou, C.; Tsigalou, C.; Bezirtzoglou, E. Towards Advances in Medicinal Plant Antimicrobial Activity: A Review Study on Challenges and Future Perspectives. *Microorganisms* **2021**, *9*, 2041.

(3) Dey, P.; Parai, D.; Banerjee, M.; Hossain, S. T.; Mukherjee, S. K. Naringin Sensitizes the Antibiofilm Effect of Ciprofloxacin and Tetracycline against Pseudomonas Aeruginosa Biofilm. *Int. J. Med. Microbiol.* **2020**, *310*, No. 151410.

(4) Kaper, J.; Nataro, J.; Mobley, H. Pathogenic Escherichia coli. *Nat. Rev. Microbiol.* **2004**, *2*, 123−140.

(5) Kashef, M. T.; Saleh, N. M.; Assar, N. H.; Ramadan, M. A. The Antimicrobial Activity of Ciprofloxacin-Loaded Niosomes against Ciprofloxacin-Resistant and Biofilm-Forming Staphylococcus aureus. *Infect. Drug Resist* **2020**, *13*, 1619−1629.

(6) Spaulding, A. R.; Satterwhite, E. A.; Lin, Y. C.; Chuang-Smith, O. N.; Frank, K. L.; Merriman, J. A.; Schaefers, M. M.; Yarwood, J. M.; Peterson, M. L.; Schlievert, P. M. Comparison of Staphylococcus aureus strains for ability to cause infective endocarditis and lethal sepsis in rabbits. *Front Cell Infect Microbiol.* **2012**, *2*, 18.

(7) Livermore, D. M.; on behalf of the British Society for Antimicrobial Chemotherapy Working Party on The Urgent Need: Regenerating Antibacterial Drug Discovery and Development; Blaser, M.; Carrs, O.; Cassell, G.; Fishman, N.; Guidos, R.; Levy, S.; Powers, J.; Norrby, R.; et al. Discovery Research: The Scientific Challenge of Finding New Antibiotics. *J. Antimicrob. Chemother.* **2011**, *66*, 1941−1944.

(8) Pugazhendhi, A.; Kumar, S. S.; Manikandan, M.; Saravanan, M. Photocatalytic Properties and Antimicrobial Efficacy of Fe Doped CuO Nanoparticles against the Pathogenic Bacteria and Fungi. *Microb. Pathog.* **2018**, *122*, 84−89.

(9) Poulson, B. G.; Alsulami, Q. A.; Sharfalddin, A.; El Agammy, E. F.; Mouffouk, F.; Emwas, A.-H.; Jaremko, L.; Jaremko, M. Cyclodextrins: Structural, Chemical, and Physical Properties, and Applications. *Polysaccharides* **2022**, *3*, 1−31.

(10) Mohammed, A. S. A.; Naveed, M.; Jost, N. Polysaccharides; Classification, Chemical Properties, and Future Perspective Applications in Fields of Pharmacology and Biological Medicine (A Review of Current Applications and Upcoming Potentialities). *J. Polym. Environ.* **2021**, *29*, 2359−2371.

(11) Das, S. S.; Kar, S.; Singh, S. K.; Verma, P. R. P.; Hussain, A.; Beg, S. Chapter 2 - Chitosan-Based Systems for Oral Drug Delivery Applications. In *Chitosan in Drug Delivery*; Academic Press, 2022, pp. 23−53.

(12) Kalliola, S.; Repo, E.; Srivastava, V.; Heiskanen, J. P.; Sirviö, J. A.; Liimatainen, H.; Sillanpää, M. The PH Sensitive Properties of Carboxymethyl Chitosan Nanoparticles Cross-Linked with Calcium Ions. *Colloids Surfaces B Biointerfaces* **2017**, *153*, 229−236.

(13) Zhang, J.; Ye, C.-Z.; Liu, Z.-Y.; Yang, Q.; Ye, Y. Preparation And Antibacterial Effects Of Carboxymethyl Chitosan-Modified Photo-

Responsive Camellia Sapogenin Derivative Cationic Liposomes. *Int. J. Nanomedicine* **2019**, *14*, 8611−8626.
(14) Tan, Y.; Han, F.; Ma, S.; Yu, W. Carboxymethyl chitosan prevents formation of broad-spectrum biofilm. *Carbohydr. Polym.* **2011**, *84*, 1365−1370.
(15) Kilicarslan, M.; Ilhan, M.; Inal, O.; Orhan, K. Preparation and Evaluation of Clindamycin Phosphate Loaded Chitosan/Alginate Polyelectrolyte Complex Film as Mucoadhesive Drug Delivery System for Periodontal Therapy. *Eur. J. Pharm. Sci. Off. J. Eur. Fed. Pharm. Sci.* **2018**, *123*, 441−451.
(16) Kurczewska, J. Recent Reports on Polysaccharide-Based Materials for Drug Delivery. *Polymers* **2022**, *14*, 4189 DOI: 10.3390/polym14194189.
(17) Yan, K.; Wan, Y.; Xu, F.; Lu, J.; Yang, C.; Li, X.; Lu, Z.; Wang, X.; Wang, D. Ionic crosslinking of alginate/carboxymethyl chitosan fluorescent hydrogel for bacterial detection and sterilization. *Carbohydr. Polym.* **2023**, *302*, No. 120427.
(18) Soni, K.; Mujtaba, A.; Akhter, M. H.; Zafar, A.; Kohli, K. Optimisation of Ethosomal Nanogel for Topical Nano-CUR and Sulphoraphane Delivery in Effective Skin Cancer Therapy. *J. Microencapsul.* **2020**, *37*, 91−108.
(19) Kausar, H.; Mujeeb, M.; Ahad, A.; Moolakkadath, T.; Aqil, M.; Ahmad, A.; Akhter, M. H. Optimization of Ethosomes for Topical Thymoquinone Delivery for the Treatment of Skin Acne. *J. Drug Delivery Sci. Technol.* **2019**, *49*, 177−187.
(20) Md, S.; Alhakamy, N. A.; Aldawsari, H. M.; Husain, M.; Khan, N.; Alfaleh, M. A.; Asfour, H. Z.; Riadi, Y.; Bilgrami, A. L.; Akhter, M. H. Plumbagin-Loaded Glycerosome Gel as Topical Delivery System for Skin Cancer Therapy. *Polymers (Basel).* **2021**, *13*, 923.
(21) Md, S.; Alhakamy, N. A.; Neamatallah, T.; Alshehri, S.; Mujtaba, M. A.; Riadi, Y.; Radhakrishnan, A. K.; Khalilullah, H.; Gupta, M.; Akhter, M. H. Development, Characterization, and Evaluation of α-Mangostin-Loaded Polymeric Nanoparticle Gel for Topical Therapy in Skin Cancer. *Gels (Basel, Switzerland)* **2021**, *7*, 230.
(22) Akhter, M. H.; Kumar, S.; Nomani, S. Sonication Tailored Enhance Cytotoxicity of Naringenin Nanoparticle in Pancreatic Cancer: Design, Optimization, and in Vitro Studies. *Drug Dev. Ind. Pharm.* **2020**, *46*, 659−672.
(23) Karim, S.; Akhter, M. H.; Burzangi, A. S.; Alkreathy, H.; Alharthy, B.; Kotta, S.; Md, S.; Rashid, M. A.; Afzal, O.; Altamimi, A. S. A.; et al. Phytosterol-Loaded Surface-Tailored Bioactive-Polymer Nanoparticles for Cancer Treatment: Optimization, In Vitro Cell Viability, Antioxidant Activity, and Stability Studies. *Gels* **2022**, *8*, 219.
(24) Shariati, A.; Arshadi, M.; Khosrojerdi, M. A.; Abedinzadeh, M.; Ganjalishahi, M.; Maleki, A.; Heidary, M.; Khoshnood, S. The Resistance Mechanisms of Bacteria against Ciprofloxacin and New Approaches for Enhancing the Efficacy of This Antibiotic. *Front. public Heal.* **2022**, *10*, No. 1025633.
(25) Tehler, U.; Fagerberg, J. H.; Svensson, R.; Larhed, M.; Artursson, P.; Bergström, C. A. S. Optimizing Solubility and Permeability of a Biopharmaceutics Classification System (BCS) Class 4 Antibiotic Drug Using Lipophilic Fragments Disturbing the Crystal Lattice. *J. Med. Chem.* **2013**, *56*, 2690−2694.
(26) Bharti, S.; Rani, N.; Krishnamurthy, B.; Arya, D. S. Preclinical Evidence for the Pharmacological Actions of Naringin: A Review. *Planta Med.* **2014**, *80*, 437−451.
(27) Manchope, M. F.; Casagrande, R.; Verri, W. A. J. Naringenin: An Analgesic and Anti-Inflammatory Citrus Flavanone. *Oncotarget* **2017**, *8*, 3766−3767.
(28) Rivoira, M. A.; Rodriguez, V.; Talamoni, G.; Tolosa de Talamoni, N. New Perspectives in the Pharmacological Potential of Naringin in Medicine. *Curr. Med. Chem.* **2021**, *28*, 1987−2007.
(29) Choi, J.-S.; Shin, S.-C. Enhanced Paclitaxel Bioavailability after Oral Coadministration of Paclitaxel Prodrug with Naringin to Rats. *Int. J. Pharm.* **2005**, *292*, 149−156.
(30) Céliz, G.; Daz, M.; Audisio, M. C. Antibacterial Activity of Naringin Derivatives against Pathogenic Strains. *J. Appl. Microbiol.* **2011**, *111*, 731−738.
(31) Han, G.; Lee, D. G. Naringin generates three types of reactive oxygen species contributing differently to apoptosis-like death in Escherichia coli. *Life Sci.* **2022**, *304*, No. 120700.
(32) Toragall, V.; Jayapala, N.; Vallikannan, B. Chitosan-oleic acid-sodium alginate a hybrid nanocarrier as an efficient delivery system for enhancement of lutein stability and bioavailability. *Int. J. Biol. Macromol.* **2020**, *150*, 578−594.
(33) Ebrahimi, M. H.; Samadian, H.; Davani, S. T.; Kolarijani, N. R.; Mogharabian, N.; Salami, M. S.; Salehi, M. Peripheral nerve regeneration in rats by chitosan/alginate hydrogel composited with Berberine and Naringin nanoparticles: in vitro and in vivo study. *J. Mol. Liq.* **2020**, *318*, No. 114226.
(34) Zhang, H.; Gu, Z.; Li, W.; Guo, L.; Wang, L.; Guo, L.; Ma, S.; Han, B.; Chang, J. PH-Sensitive O-Carboxymethyl Chitosan/Sodium Alginate Nanohydrogel for Enhanced Oral Delivery of Insulin. *Int. J. Biol. Macromol.* **2022**, *223*, 433−445.
(35) Afzal, O.; Akhter, M. H.; Ahmad, I.; Muzammil, K.; Dawria, A.; Zeyaullah, M.; Altamimi, A. S. A.; Khalilullah, H.; Mir Najib Ullah, S. N.; Rahman, M. A.; et al. A β-Sitosterol Encapsulated Biocompatible Alginate/Chitosan Polymer Nanocomposite for the Treatment of Breast Cancer. *Pharmaceutics* **2022**, *14*, 1711.
(36) Alhalmi, A.; Amin, S.; Beg, S.; Al-Salahi, R.; Mir, S. R.; Kohli, K. Formulation and Optimization of Naringin Loaded Nanostructured Lipid Carriers Using Box-Behnken Based Design: In Vitro and Ex Vivo Evaluation. *J. Drug Delivery Sci. Technol.* **2022**, *74*, No. 103590.
(37) Wang, J.; Ye, X.; Lin, S.; Liu, H.; Qiang, Y.; Chen, H.; Jiang, Z.; Zhang, K.; Duan, X.; Xu, Y. Preparation, Characterization and in Vitro and in Vivo Evaluation of a Solid Dispersion of Naringin. *Drug Dev. Ind. Pharm.* **2018**, *44*, 1725−1732.
(38) Rizvi, S. S. B.; Akhtar, N.; Minhas, M. U.; Mahmood, A.; Khan, K. U. Synthesis and Characterization of Carboxymethyl Chitosan Nanosponges with Cyclodextrin Blends for Drug Solubility Improvement. *Gels* **2022**, *8*, 55.
(39) Isa, T.; Zakaria, Z. A. B.; Rukayadi, Y.; Mohd Hezmee, M. N.; Jaji, A. Z.; Imam, M. U.; Hammadi, N. I.; Mahmood, S. K. Antibacterial Activity of Ciprofloxacin-Encapsulated Cockle Shells Calcium Carbonate (Aragonite) Nanoparticles and Its Biocompatability in Macrophage J774A.1. *Int. J. Mol. Sci.* **2016**, *17*, 713.
(40) S, M.; Iyer, P. R. Naringin Loaded Chitosan Nanoparticle for Bone Regeneration: A Preliminary in Vitro Study. *J. Nanomed. Nanotechnol.* **2018**, *9*, No. 1000507.
(41) Torge, A.; Wagner, S.; Chaves, P. S.; Oliveira, E. G.; Guterres, S. S.; Pohlmann, A. R.; Titz, A.; Schneider, M.; Beck, R. C. R. Ciprofloxacin-Loaded Lipid-Core Nanocapsules as Mucus Penetrating Drug Delivery System Intended for the Treatment of Bacterial Infections in Cystic Fibrosis. *Int. J. Pharm.* **2017**, *527*, 92−102.
(42) Ghaffari, S.; Varshosaz, J.; Haririan, I.; Khoshayand, M. R.; Azarmi, S.; Gazori, T. Ciprofloxacin Loaded Alginate/Chitosan and Solid Lipid Nanoparticles, Preparation, and Characterization. *J. Dispers. Sci. Technol.* **2012**, *33*, 685−689.
(43) Khan, Y. A.; Ozaltin, K.; Bernal-Ballen, A.; Di Martino, A. Chitosan-Alginate Hydrogels for Simultaneous and Sustained Releases of Ciprofloxacin, Amoxicillin and Vancomycin for Combination Therapy. *J. Drug Delivery Sci. Technol.* **2021**, *61*, No. 102126.
(44) Eltaweil, A. S.; Ahmed, M. S.; El-Subruiti, G. M.; Khalifa, R. E.; Omer, A. M. Efficient Loading and Delivery of Ciprofloxacin by Smart Alginate/Carboxylated Graphene Oxide/Aminated Chitosan Composite Microbeads: In Vitro Release and Kinetic Studies. *Arab. J. Chem.* **2023**, *16*, No. 104533.
(45) Wang, Y.; Wen, B.; Yu, H.; Ding, D.; Zhang, J.; Zhang, Y.; Zhao, L.; Zhang, W. Berberine Hydrochloride-Loaded Chitosan Nanoparticles Effectively Targets and Suppresses Human Nasopharyngeal Carcinoma. *J. Biomed. Nanotechnol.* **2018**, *14*, 1486−1495.
(46) Thai, H.; Thuy Nguyen, C.; Thi Thach, L.; Thi Tran, M.; Duc Mai, H.; Thi Thu Nguyen, T.; Duc Le, G.; Van Can, M.; Dai Tran, L.; Long Bach, G.; et al. Characterization of Chitosan/Alginate/Lovastatin Nanoparticles and Investigation of Their Toxic Effects in Vitro and in Vivo. *Sci. Rep.* **2020**, *10*, 909.

https://doi.org/10.1021/acsomega.3c08200
ACS Omega 2024, 9, 6845−6860

(47) Farheen, M.; Akhter, M. H.; Chitme, H.; Suliman, M.; Jaremko, M.; Emwas, A.-H. Surface-Modified Biobased Polymeric Nanoparticles for Dual Delivery of Doxorubicin and Gefitinib in Glioma Cell Lines. *ACS Omega* **2023**, *8*, 28165−28184.
(48) Bagre, A. P.; Jain, K.; Jain, N. K. Alginate Coated Chitosan Core Shell Nanoparticles for Oral Delivery of Enoxaparin: In Vitro and in Vivo Assessment. *Int. J. Pharm.* **2013**, *456*, 31−40.
(49) Alhalmi, A.; Amin, S.; Khan, Z.; Beg, S.; Al, O.; Saleh, A.; Kohli, K. Nanostructured Lipid Carrier-Based Codelivery of Raloxifene and Naringin: Formulation, Optimization, In Vitro, Ex Vivo, In Vivo Assessment, and Acute Toxicity Studies. *Pharmaceutics* **2022**, *14*, 1771.
(50) Dobrovolskaia, M. A.; Clogston, J. D.; Neun, B. W.; Hall, J. B.; Patri, A. K.; McNeil, S. E. Method for Analysis of Nanoparticle Hemolytic Properties in Vitro. *Nano Lett.* **2008**, *8*, 2180−2187.
(51) Gerçek, E.; Zengin, H.; Erdem Erişir, F.; Yılmaz, Ö. Biochemical Changes and Antioxidant Capacity of Naringin and Naringenin against Malathion Toxicity in Saccharomyces Cerevisiae. *Comp. Biochem. Physiol. Part C Toxicol. Pharmacol.* **2021**, *241*, No. 108969.
(52) Imam, S. S.; Gilani, S. J.; Zafar, A.; Jumah, M. N.; Ali, R.; Ahmed, M. M.; Alshehri, S. Preparation and Optimization of Naringin Oral Nanocarrier: In Vitro Characterization and Antibacterial Activity. *Coatings* **2022**, *12*, 1230 DOI: 10.3390/coatings12091230.
(53) Moore, T. L.; Rodriguez-Lorenzo, L.; Hirsch, V.; Balog, S.; Urban, D.; Jud, C.; Rothen-Rutishauser, B.; Lattuada, M.; Petri-Fink, A. Nanoparticle Colloidal Stability in Cell Culture Media and Impact on Cellular Interactions. *Chem. Soc. Rev.* **2015**, *44*, 6287−6305.
(54) Katuwavila, N. P.; Perera, A. D. L. C.; Samarakoon, S. R.; Soysa, P.; Karunaratne, V.; Amaratunga, G. A. J.; Karunaratne, D. N. Chitosan-Alginate Nanoparticle System Efficiently Delivers Doxorubicin to MCF-7 Cells. *J. Nanomater.* **2016**, *2016*, No. 3178904.
(55) Chou, T.-C. Drug combination studies and their synergy quantification using the Chou−Talalay method. *Cancer Res.* **2010**, *70*, 440−446.
(56) Soliman, N. M.; Shakeel, F.; Haq, N.; Alanazi, F. K.; Alshehri, S.; Bayomi, M.; Alenazi, A. S. M.; Alsarra, I. A. Development and Optimization of Ciprofloxacin HCl-Loaded Chitosan Nanoparticles Using Box-Behnken Experimental Design. *Molecules* **2022**, *27*, 4468.
(57) Sobhani, Z.; Samani, S. M.; Montaseri, H.; Khezri, E. Nanoparticles of Chitosan Loaded Ciprofloxacin: Fabrication and Antimicrobial Activity. *Adv. Pharm. Bull.* **2017**, *7*, 427−432.
(58) Mohsen, E.; El-Borady, O. M.; Mohamed, M. B.; Fahim, I. S. Synthesis and Characterization of Ciprofloxacin Loaded Silver Nanoparticles and Investigation of Their Antibacterial Effect. *J. Radiat. Res. Appl. Sci.* **2020**, *13*, 416−425.
(59) Toragall, V.; Jayapala, N.; S, P. M.; Vallikanan, B. Biodegradable Chitosan-Sodium Alginate-Oleic Acid Nanocarrier Promotes Bioavailability and Target Delivery of Lutein in Rat Model with No Toxicity. *Food Chem.* **2020**, *330*, No. 127195.
(60) Ansari, M. J.; Rahman, M.; Alharbi, K. S.; Altowayan, W. M.; Ali, A. M. A.; Almalki, W. H.; Barkat, M. A.; Singh, T.; Nasar, S.; Akhter, M. H.; et al. Hispolon-Loaded Liquid Crystalline Nanoparticles: Development, Stability, In Vitro Delivery Profile, and Assessment of Hepatoprotective Activity in Hepatocellular Carcinoma. *ACS Omega* **2022**, *7*, 9452−9464.
(61) Sharma, J. B.; Bhatt, S.; Tiwari, A.; Tiwari, V.; Kumar, M.; Verma, R.; Kaushik, D.; Virmani, T.; Kumar, G.; Al kamaly, O.; et al. Statistical Optimization of Tetrahydrocurcumin Loaded Solid Lipid Nanoparticles Using Box Behnken Design in the Management of Streptozotocin-Induced Diabetes Mellitus. *Saudi Pharm. J.* **2023**, *31*, No. 101727.
(62) Farheen, M.; Akhter, M. H.; Chitme, H.; Akhter, M. S.; Tabassum, F.; Jaremko, M.; Emwas, A.-H. Harnessing Folate-Functionalized Nasal Delivery of Dox–Erlo-Loaded Biopolymeric Nanoparticles in Cancer Treatment: Development, Optimization, Characterization, and Biodistribution Analysis. *Pharmaceuticals* **2023**, *16*, 207 DOI: 10.3390/ph16020207.
(63) Gabriele, M.; Caddeo, C.; Lubrano, V.; Valenti, D.; Pucci, L. Encapsulation of Bioactive Fermented Wheat (Lisosan G) in Eudragit-Liposomes. *LWT* **2022**, *156*, No. 113044.

https://doi.org/10.1021/acsomega.3c08200
ACS Omega 2024, 9, 6845−6860